Cortical Processing of Visual Parts and Wholes

Stephanie Marie Roldán

Thesis submitted to the faculty of the Virginia Polytechnic Institute and State University in partial fulfillment of the requirements for the degree of

Master of Science
In
Psychology

Anthony Cate, Chair
Rachel Diana
David Harrison

August 25, 2014
Blacksburg, Virginia

Keywords: object recognition, visual perception, visual crowding, holistic processing, configural processing

Cortical Processing of Visual Parts and Wholes

Stephanie M. Roldán

ABSTRACT

Visual perception theory distinguishes between two distinct levels of object processing: holistic, based on global shape, and configural, based on local features and/or component parts. Empirical evidence suggests that different cortical regions may support these levels; holistic processing correlates with activation in the lateral occipital-temporal cortex (LOC), whereas configural processes correspond to activation in the parietal lobe, particularly the intraparietal sulcus (IPS). This study combined theories of visual part structure with neuroimaging methods to investigate the relative contribution of holistic and configural processing in an ecologically valid object recognition task. Rather than rely on stimuli specifically designed to evoke holistic or configural processing, this study used photographs of objects selected without *a priori* assumptions concerning physical part structure. Twenty participants viewed objects at fixation while undergoing fMRI, followed by a behavioral object identification task involving the same objects presented in peripheral vision. Behavioral data were analyzed according to theories of visual crowding to yield an objective estimate of the number of parts perceived within each object. Neuroimaging results revealed increased activation for holistic objects containing fewer parts in the right parietal lobe and superior temporal gyrus and bilaterally in the fusiform gyrus, suggesting a relation between holistic processing areas and object perception. Configural objects with many parts elicited increased activation in the left angular gyrus. This study, to our knowledge, is the first to investigate the cortical visual regions involved when observers engage in holistic and configural processing as a natural part of visual recognition.

ACKNOWLEDGEMENTS

I would like to take this opportunity to extend my deepest gratitude to my colleagues, friends, and family, without whom this work would not have been accomplished. First and foremost, I would like to thank my advisor, Dr. Anthony Cate, for giving me the opportunity to learn from him and work together here at Virginia Tech. Thank you for sharing your knowledge, support, and enthusiasm for research with me. Your encouragement and guidance has helped me through this project even when I had my doubts. I am also very grateful to my committee members, Dr. Rachel Diana and Dr. David Harrison, for sharing your unique perspectives on this research and helping me to expand the way I view and understand this field.

In addition, my sincerest appreciation goes out to the members of the Visual Neuroscience Lab who voluntarily spent many hours with me at the scanner during data collection. I wouldnôt have a study without your help.

To my friends and family, both near and far, thank you for your unwavering support and faith. I would especially like to thank my father for his immeasurable encouragement and for constantly cheering me on in my endeavors. To my mother and sister, thank you both for believing in me and offering a kind word or a laugh when I needed them most. I would also like to thank Aschvin Chawan for helping me every step of the way and reminding me to stay calm and cool-headed throughout this process. Finally, I cannot thank my friends enough for the love and support they have given me over the years. I am blessed to have you all in my life and I am forever grateful to each and every one of you.

Table of Contents

List of Figures

List of Tables

Cortical Processing of Visual Parts and Wholes

Despite extensive research in the cognitive neuroscience of vision, a clear explanation of how the brain interprets visual input to result in the recognition of a named object remains elusive. Although studies have revealed general systems recruited during visual processing of objects, much remains unclear as to how visual information is represented and interpreted at the neural level.

Visual Processing Theory of Object Parts and Wholes

A long-standing debate exists among visual neuroscientists regarding the features most useful in object perception. While some emphasize the specialized role of holistic processing based on global shapes and relationships amongst features (Tanaka & Farah, 1993), others argue that individual details contain the most important information for recognition (Pomerantz, Sager, & Stoever, 1977). These modes of visual processing - henceforth referred to as *holistic* and *configural processing*, respectively - have been implicated in recognition tasks involving a wide range of salient stimuli, including faces (Farah, Tanaka, & Drain, 1995; Richler, Cheung, & Gauthier, 2011), whole body postures (Reed, Stone, Grubb, & McGoldrick, 2006), and letters (Pelli, Farell, & Moore, 2003; Pelli & Tillman, 2007). Many researchers interpret the results of such studies to suggest that each processing system is uniquely attuned to perceive certain categories of stimuli. It is important to note, however, that these viewpoints are not mutually exclusive; it is indeed possible that both processing techniques may be involved in the same task depending on the stimulus under observation (Martelli, Majaj, & Pelli, 2005).

Neural Correlates of Configural and Holistic Processing

Although object parts and wholes are innately intertwined in visual perception, there is substantial empirical evidence to suggest that global shapes and their individual features contribute uniquely to perceptive processes even at the cognitive level. Note here that this study defines the term *feature* as an independently recognized, discrete component of an image (Suchow & Pelli, 2013). However, the relationship between part and whole representations can be difficult to disentangle, considering that the perception of one is influenced heavily by the perception of the other. For example, the results of several studies have indicated an apparent advantage for identifying individual features within the context of a whole as opposed to in isolation (Kubilius, Wagemans, & Beeck, 2011; Pomerantz, Sager, & Stoever, 1977). This trend

is commonly known as the *configural-superiority effect* and should not be confused with the current documentôs use of the term ñconfiguralò to mean ñparts-basedò processing. Rather, the configural superiority effect refers to the enhanced ability to identify attributes of individual features when they are presented within a larger whole (given that the extra information is constant between all compared samples), as opposed to when the feature appears by itself (Pomerantz & Cragin, 2012). This finding is one of many that have provided the source of continuous debate regarding the role and representation of parts-based information and its contributions to the recognition of global shapes, and it serves to illustrate the unique challenges in distinguishing the role of parts and wholes in object perception at the cognitive-behavioral level.

However, brain activation revealed by functional magnetic resonance imaging (fMRI) during visual recognition tasks has further illuminated the processes involved in part and whole perception and the neural regions associated with each. In an investigation of the configural superiority effect, Kubilius, Wagemans, and Beeck (2011) examined neural activity associated with identifying features of a single stimulus (a straight line) when presented in isolation and when viewed within the context a configural shape (a corner bisected by the target line). Their results showed that parts were represented mostly in the early, retinotopically-organized visual areas of the brain while whole shapes were associated with activation in the lateral occipital cortex (LOC). The LOC receives input regarding low-level sensory information from the early visual areas located in the occipital lobe - primary visual cortex (V1), V2, and V3 - and is therefore considered a high-level visual area associated with increased perceptual interpretation (Grill-Spector & Malach, 2004). In their study, a computer program was trained to classify fMRI responses as belonging to either parts or wholes experimental conditions. Based on the yielded pairwise comparisons, it was found that the representation of global shapes was easier to detect in LOC but not in early visual areas, whereas whole shapes could not be reliably reconstructed from the parts represented in early visual areas (V1-V3) alone (Kubilius, Wagemans, & Beeck, 2011). This dissociation between part and whole representations suggests that each type of information is perceived in separate regions of the brain that employ fundamentally distinct processing mechanisms. Several other studies have also found selective activation for whole shapes in LOC (Grill-Spector et al., 1998; Kourtzi & Kanwisher, 2001; Malach et al., 1995), which strengthens in intensity in the ventral occipital-temporal object areas (Lerner, Hendler,

Ben-Bashat, Harel, & Malach, 2001). Finally, the observed integrative nature of this region further supports the theory that it may play a critical role in the mediation of global shape processing (Lerner, Hendler, & Malach, 2002).

Due to the interdependent nature of component parts in whole objects, the intermediary processes associated with parts-based representation and interpretation are slightly more difficult to tease apart than those involved with whole objects. However, through the use of careful design methods, several studies have discovered cortical areas that appear to be specifically involved in configural perception. As mentioned above, parts were more successfully decoded from activation in early visual areas than in LOC (Kubilius, Wagemans, & Beeck, 2011). Furthermore, another study found reduced neural activation in the inferior intraparietal sulcus (IPS) as individual objects were grouped together (Xu & Chun, 2007). This sensitivity of the IPS to the grouping of individual components suggests that it is involved in encoding parts-based information. In addition, patients with bilateral parietal damage exhibit increased difficulty in recognizing inanimate objects based on their unique parts (Riddoch & Humphreys, 2004), implicating the parietal lobe in the perception of local features. In order to better relate the role of component parts to global shape processing, Lerner, Hendler, Ben-Bashat, Harel, and Malach (2001) proposed a posterior-anterior hierarchical axis of object processing that progresses from early visual areas to the dorsal side of the lateral-occipital sulcus. In their study, early visual areas through retinotopic areas V4/V8 were less sensitive to the progressive segmentation and scrambling of whole-object images than the LOC, suggesting that these early visual regions recruited less holistic processing mechanisms. This framework, combined with reported findings from other studies, implicates early visual areas and parietal lobe activity (particularly the IPS) in parts-based processing, which then transitions to more holistic processing as sensory input progresses anteriorly toward the regions of the LOC and ventral occipital temporal cortex.

Hemispheric Differences in Object Recognition

The perception of holistic and configural objects may also be affected by differential recruitment of one cerebral hemisphere over another. Some empirical studies suggest that the level of shape to which humans attend is lateralized between the two hemispheres of the brain (Delis, Robertson, & Efron, 1986; Robertson, Lamb, & Knight, 1988). In right-handed individuals, the left hemisphere often exhibits local feature bias whereas the right hemisphere is typically biased toward global shape perception - a trend which is reversed in left-handers

(Mevorach, Humphreys, & Shalev, 2005). This lateralized effect is especially robust in patients with unilateral brain lesions. When presented with objects containing distinct local and global features, subjects with large lesions in the right hemisphere experience difficulty in identifying global forms, whereas subjects with left hemisphere lesions show poorer responses to local features (Robertson, Lamb, & Knight, 1988). These deficits were found to be related to perceptual mechanisms mediated by the superior temporal gyrus and were not attributable to controlled attentional processes alone (Robertson, Lamb, & Knight, 1988). Indeed, evidence of these impairments remained during recall tasks in which subjects were asked to recreate the image they previously viewed (Delis, Robertson, & Efron, 1986), further supporting the perceptual basis of the lateralization effect.

This contrast between the functions of either hemisphere in the identification of local and global features may carry important implications for object perception. For example, it has been proposed that the two hemispheres operate within an interconnected network to mediate the perception of parts and wholes during object recognition (Robertson & Lamb, 1991). Furthermore, the hemispheric laterality of holistic and configural processing offers an opposing argument to the commonly held perspectives that part and whole perception are mutually exclusive, hierarchical, or asynchronous; in the framework of hemispheric specialization, it is possible that both types of information are processed simultaneously but in different hemispheres of the brain (Robertson & Lamb, 1991).

However, not all empirical findings support the existence of hemispheric lateralization in visual perception. A meta-analysis found that, of the studies that reported hemispheric bias, the most commonly found advantage was for the left hemisphere (right visual field) only; very few articles reported both left and right lateral biases, and some reported none at all (Yovel, Yovel, & Levy, 2001). Based on an examination of study designs and stimulus types, the authors concluded that asymmetries were more likely to be apparent in divided- rather than focused-attention tasks that include stimuli with equally salient global and local levels. This is because the common trend toward *global salience* (related to the configural superiority effect) may negate the advantage for local feature processing, thus attenuating the strength of its effects.

Luckily, it is relatively simple to test the effects of hemispheric processing during behavioral tasks. Due to the contralateral organization of the visual system, input from the left half of the visual field is projected to the right hemisphere and vice versa (Sperry, 1968). This

structural system provides a simple yet effective means to examine lateralized differences in configural and whole perception; by presenting visual stimuli to only one half of the visual field at a time, behavioral responses may be compared across conditions and analyzed for bias. Additionally, with the use of neuroimaging methods, neural responses can be analyzed within each hemisphere independently even when stimuli are presented at fixation. Although it is often difficult to precisely determine the nature of the interaction between hemispheres, these techniques have the potential to illuminate the role of hemispheric differences in visual perception.

Visual Crowding

In order to infer how visual sensory information is detected and interpreted during object recognition at the behavioral level, many researchers take advantage of a visual phenomenon known as *crowding*. Crowding describes the effect of clutter that results in an impaired ability to discriminate visual details and, consequently, recognition for images presented in the peripheral visual field (Pelli & Tillman, 2008; Whitney & Levi, 2011). This effect can be observed naturally in any scene in which two or more items appear in close proximity to one another. Though it is easy to distinguish amongst closely-spaced, separate objects when viewed at *fixation* (i.e., when the image is centered on the retina), the same objects become blurry, jumbled, and undefined when observed in peripheral vision.

The crowding effect is uniquely informative for perceptual research due to the specific manner in which it impairs object recognition. Degradation of object recognition is known to be directly related to the proximity of a target stimulus to extraneous visual information called *flankers* (Whitney & Levi, 2011). The resulting conflict stems directly from a physical limitation imposed by the cortical organization of the visual processing system. Visual input projects retinotopically onto V1 such that adjacent neurons in the brain respond to adjacent observed stimuli (Tootell, Silverman, Switkes, & Valois, 1982). However, the neural activation elicited in V1 does not bear a 1:1 correspondence with the image or scene under observation. Instead, neural response in V1 and several other human visual areas is distorted logarithmically, originating from the area that detects input from the fovea to those that receive signals from the outer periphery of the visual field (Pelli, 2008). In other words, the most direct correspondence between real-world images and cortical activation occurs at the center of vision and becomes increasingly distorted as it moves outward to the peripheral visual field. This organization,

combined with the fact that the amount of cortex dedicated to processing visual information from the fovea is relatively greater than the amount used for the remaining visual field ï an effect known as *cortical magnification* (Dougherty et al., 2003; Van Essen, Newsome, & Maunsell, 1984) ï is the reason why clearest, sharpest vision occurs at the area of fixation and steeply falls off as it moves toward the outer edge of the visual field. These factors directly contribute to the crowding phenomenon, as the ability for neurons to accurately represent and distinguish similar shapes declines sharply outside of the area of fixation. In addition, crowding is distinct from *acuity*, or the ability to detect fine details, in the manner in which it degrades recognition. Simply put, acuity is limited by size, whereas crowding is limited by spacing amongst shapes. Therefore, in the case of crowding, the distance from the center of one shape to the center of another, regardless of the size of the stimulus, has the greatest influence on recognition (Song, Levi, & Pelli, 2014).

The specific psychophysical nature of crowding allows a better understanding of the manner in which visual information is represented at the neural level, and thus how the crowding effect relates to the cognitive perception of stimuli. Based on knowledge of crowding mechanisms, a group of researchers calculated the minimum spatial separation necessary for an object to be recognized at various locations in the visual field when flanked by distractors. This distance, called the *critical spacing*, was found to be roughly half the eccentricity of the object from fixation (Bouma, 1970; Pelli, 2008). The term *isolation field* was coined for the region described by a perimeter of critical spacing around an object. According to the researchersô proposed formula, as target objects and their flankers move farther into the peripheral field ï that is, as their eccentricity from fixation increases - the amount of space between the target and flankers required to successfully distinguish amongst objects also increases. This rule of minimum critical distance is even said to be generalizable across all sizes and categories of object stimuli (Martelli, Majaj, & Pelli, 2005; Pelli, 2008). Based on this research, recognition fails when 1) critical spacing is not met and/or 2) features within an object are integrated within an isolation field that is inappropriately large, due to the large size limitation of isolation fields in peripheral vision (Pelli, Palomares, & Majaj, 2004). These reliable, objectively measurable attributes of crowding therefore make it a useful tool for inferring the contribution of specific visual information during object recognition.

In addition to the detection of a single whole object that appears near a flanker, crowding is proposed to operate similarly within an individual object presented alone (Pelli, 2008). In this scenario, the various features contained within an object potentially serve as their own flankers. By applying crowding theory to parts-based processing of single objects, it has been posited that if an object has many parts, these parts will crowd each other at high eccentricities in peripheral vision and thus prevent recognition (Martelli, Majaj, & Pelli, 2005; Pelli & Tillman, 2008). Conversely, images processed as having one or few parts would not experience crowding and would therefore be identifiable at greater eccentricity from fixation. Given that simple steps are taken to ensure that low retinal acuity in the periphery is not at play, it could then be possible to identify the maximum eccentricity at which an object can be recognized and use this distance to infer the number of parts it contains (Martelli, Majaj, & Pelli, 2005; Pelli & Tillman, 2008). This type of measure would provide a direct and objective means for assessing whether an object has been recognized via holistic or configural processing, such that the fewer parts, the more holistic the recognition process. It is upon this framework of intra-object crowding that the current study draws in order to investigate how the visual system detects and combines distinct features in order to perceive objects.

Methods

Intra-object crowding and its neural correlates were investigated in a two-part experiment that involved viewing and identifying photographs of real-world objects. Participants completed a neuroimaging session in the fMRI scanner followed by a behavioral object identification task no more than one week later. Measurements collected during behavioral testing were used within- and between-subjects to inform the analysis of the neuroimaging data.

Participants

Twenty volunteers (9 female, 11 male) were recruited from the Virginia Tech campus and surrounding community and received monetary compensation ($40/hour) for their time. The mean age of participants was 23.55 years, with a median age of 23. One participant was left-handed and one reported ambidexterity but used their right hand during experimental tasks; both were males. All participants reported normal or corrected-to-normal vision and were instructed to wear their glasses or contacts during the study if they needed to see clearly at short distances. When necessary, MRI-safe glasses with prescription lenses were used during the neuroimaging

portion of the experiment. Of the 20 total participants, 2 were excluded from the neuroimaging analysis due to a loss of time-locked experimental data related to the neuroimaging task and 1 due to irregular data. However, the intact behavioral task data for each of these participants was retained in relevant analyses. Of the 17 participants (9 female, 8 male) included in the neuroimaging analyses, the mean age was 23.44 years with a median age of 23.

Informed Consent

A consent form including a detailed description of experimental procedures, rights of the participant, possible risks and benefits, and compensation was provided prior to both phases of the experiment. The form was explained verbally and subjects were given ample time to read the document and ask any questions before choosing to sign it. Participants were made aware that they had the right to withdraw from the study at any time without penalty.

Stimuli

Visual stimuli consisted of 27 object images selected from the Bank of Standardized Stimuli image database (BOSS; Brodeur, Dionne-Dostie, Montreuil, & Lepage, 2010), a collection of high-resolution photographs of real-world objects with transparent backgrounds. The BOSS dataset includes normalized data regarding the visual and semantic properties of nearly 500 images. BOSS ratings for the stimuli used in this study can be found in Appendix A. The quality of the database allows comparisons between high-level visual properties and behavioral responses. Furthermore, the diverse and well-processed photographs capture a broad range of local visual features. Stimuli chosen for this experiment were considered to be reasonably typical examples of items commonly found in the United States. In addition, selected stimuli spanned a variety of categories including living/non-living, manipulability, and visual distinctiveness. An analysis performed on data collected during a preliminary experiment using BOSS images indicated that the viewing angle of the photographed stimulus may present a possible confound for recognition (for a summary of these preliminary behavioral studies, see Appendices B & C). Therefore, only images subjectively rated to exhibit the same viewpoint with no perspective distortion were used in the current study. Due to differences in screen size and viewing distance, images subtended a visual angle no greater than 7.33° at fixation in the behavioral task and 4.29° in neuroimaging presentations. Stimuli were converted to grayscale to eliminate color cues and preprocessed using the SHINE toolbox (Willenbockel et al., 2010) to normalize for luminance and contrast. Experimental stimuli, as they appeared in the study, are

provided in Appendix D. Object images and instructions were displayed against a black background with white text when appropriate. Stimuli were presented using MATLAB (Mathworks) and Psychophysics Toolbox (Version 3; Brainard, 1997) software.

Neuroimaging

Scanning Parameters. Brain MRI scans were collected at the Virginia Tech Corporate Research Center using a 3T Siemens Tim Trio Scanner equipped with a 12-channel head coil. Foam padding provided additional support and served to minimize head movement during scanning. Headphones were provided to allow communication between the participant and the experimenter as well as attenuate acoustic noise produced by the scanner. Anatomical images were acquired with an MPRAGE sequence (voxel size = .475 x .475 x .95). Gradient echoplanar imaging (EPI) sequences were employed to collect functional data (TR = 2.26 s, TE = 25 ms). Each functional volume consisted of 42 slices with a voxel size of 3.44 x 3.44 x 3.4 and a matrix size of 64 x 64 x 42. There were no gaps between slices and the flip angle was set to 90°.

Procedure. A fast event-related fMRI design was employed to study neural activity associated with the presentation of different objects. After providing informed consent and successfully clearing the MRI safety screening criteria, an initial localizer scan was collected, followed by a high-resolution anatomical MPRAGE scan before beginning experimental trials. During experimental trial blocks, subjects viewed experimental stimuli while undergoing fMRI (visual angle no greater than 4.29°). Participants were first presented with a small, white fixation cross over a dark gray square of equal size at the center of the testing screen and were instructed to focus their attention on this cross at all times. Once every TR (TR = 2.26 s), an object image appeared directly behind the fixation stimulus for 1.5 s, thereby allowing a 0.76 s interstimulus interval, during which only the fixation cross remained on screen. At the time the object appeared, the fixation cross simultaneously changed color from white to either bright yellow or a slightly darker yellow. To facilitate passive processing of the object and avoid confounds of attention, participants were asked to monitor these color changes and respond by pressing one of two buttons to indicate which color was displayed. These button presses were recorded and primarily used to verify that the participant was awake, alert, and not focusing on the stimulus image itself. Once the object stimulus was removed from the screen, the fixation cross returned to white until the next image appeared.

Presentation order of stimuli was counterbalanced using a Type 1, Index 1 sequence which ensured that every object was preceded equally often by every other object in the stimulus set (Aguirre, 2007). This counterbalancing was essential for distinguishing the main effect of each image while controlling for carry-over effects caused by the stimuli preceding each object. In order to achieve this, null-condition stimuli consisting of a black screen with the fixation cross still visible were interspersed among the target stimuli. During these null trials, the fixation cross underwent a color change and the participant was expected to complete a button press as they would during an experimental trial. A presentation sequence was created using a web-based Type 1, Index 1 sequence generator (Aguirre, 2012) that searches among many permutations of stimulus order to identify an optimal choice given the relevant design parameters. The stimulus sequence, with individual images represented by the numbers 1-27, appears in Appendix E and was calculated to have an efficiency value of 0.39. This measure represents the ñproportion of neural variance that passes through the hemodynamic response function,ò and appeared to fall within a reasonable optimal range for a stimulus set of this size and type (Aguirre, 2009). Total scanning time averaged approximately 45 min, divided into 6 runs of about 5.5 min each in order to avoid subject fatigue. In addition, a second 6-min anatomical MPRAGE scan was collected at the end of the scanning session. Prior to collecting neuroimaging data, several null practice trials were presented using the same timing as the experimental trials. This allowed participants to become familiar with the timing of the fixation cross changes and to practice coordinating their button presses. Any questions regarding instructions were also addressed at this time. In between trial blocks, participants were allowed to rest for as long as they felt was necessary and given the option to exit the scanner if they so desired.

Behavioral Task

The behavioral phase was conducted 1-7 days following the completion of the fMRI scan and consisted of two sequential tasks.

Naming task. After providing written informed consent, participants were asked to sit in front a computer and enter basic information including age, gender, and dominant handed-ness. Subjects were then instructed to provide names for each of the experimental stimuli. Stimuli were displayed on a 24-inch LCD Dell monitor in random order at a size of 150 x 150 pixels (no greater than 7.33° visual angle) with an input dialog below them. Participants were asked to type in the name by which they felt most comfortable identifying the displayed object. To ensure

reliable naming, each image reappeared randomly until it had been labeled consistently twice in a row. These labels were used to assess the accuracy of responses during the subsequent identification task.

Critical eccentricity task. After naming all of the stimuli, participants were then instructed to use a chinrest adjusted to a comfortable height and fixate the center of the computer monitor. The chinrest served to minimize head movement and ensure that all participants viewed the screen from a standardized distance of approximately 32 cm. To prevent saccadic eye movements toward the stimulus (Becker & Fuchs, 1969), object images appeared for 150 ms on the left or right side of the screen in a pseudo-random order that prevented stimuli from appearing more than 3 times sequentially on the same side. Presenting stimuli on either side of the screen at random not only prevented participants from attempting to fixate on the object, but also allowed for the investigation of hemispheric differences in visual processing (Sperry, 1968). A small white fixation cross at the center of the screen preceded image presentation by 2000 ms. All images began at the highest eccentricity of 31.02° (650 px) from fixation and moved closer to fixation until they were correctly identified. Participants were instructed to verbally identify the object after each stimulus presentation. The experimenter coded participantsô verbal responses as correct/incorrect in real time according to the labels entered during the Naming task. In addition, subjects had the option to decline guessing the objectôs identity, in which case the response was coded as incorrect. Following an incorrect response, an image appeared 75 px (3.67°) closer to fixation when it next appeared on that side of the screen. Following a correct response, the position of the image on the screen was recorded as a measure of the *critical eccentricity*, or the minimum distance necessary to accurately identify the stimulus. Objects remained in the cycle and moved closer to fixation until they were correctly identified on both sides of the screen. So long as an object was consistently correctly identified on one side of the screen, it remained stationary in subsequent trials while the object on the opposite side continued to move closer to fixation until it, too, was correctly identified. If a previously correctly identified object was incorrectly labeled in a subsequent trial, it resumed its path toward fixation.

Hypotheses

This study draws on theories of holistic and configural processing and crowding mechanisms to investigate the relationship between visual information, its role in object

perception, and how it is represented in the human brain. As demonstrated in previous preliminary studies (Appendix C), the behavioral task was expected to reveal a continuous range of varying critical eccentricities for the stimulus set unrelated to higher-level semantic properties (Appendix B). These eccentricity measures were then used to categorize a set of normalized photographs of real-world objects as possibly containing few or many composite parts and formed the basis of fMRI analysis. Our hypotheses related to the neuroimaging experiment were as follows:

1. As indicated by the existing literature, the LOC in the ventral occipital-temporal stream was expected to show higher activation during the presentation of objects that were perceived holistically.
2. In accordance with the posterior-anterior hierarchy proposed by Lerner and colleagues (2001), holistic shapes were predicted to elicit more general activation in the ventral occipital-temporal stream, particularly in the more anterior regions of the stream.
3. Configural objects were expected to correlate with increased activity in the parietal lobe; particularly, the IPS, which has been shown to respond to manipulations in number of objects under observation (Xu & Chun, 2007).
4. In addition to these specific brain regions, the effect of holistic or configural processing was predicted to be more pronounced or even present in one hemisphere or the other. Specifically, the left hemisphere was expected to be more closely associated with parts-based processing and the right hemisphere with global shape processing (Delis, Robertson, & Efron, 1986).

Results

Behavioral Data

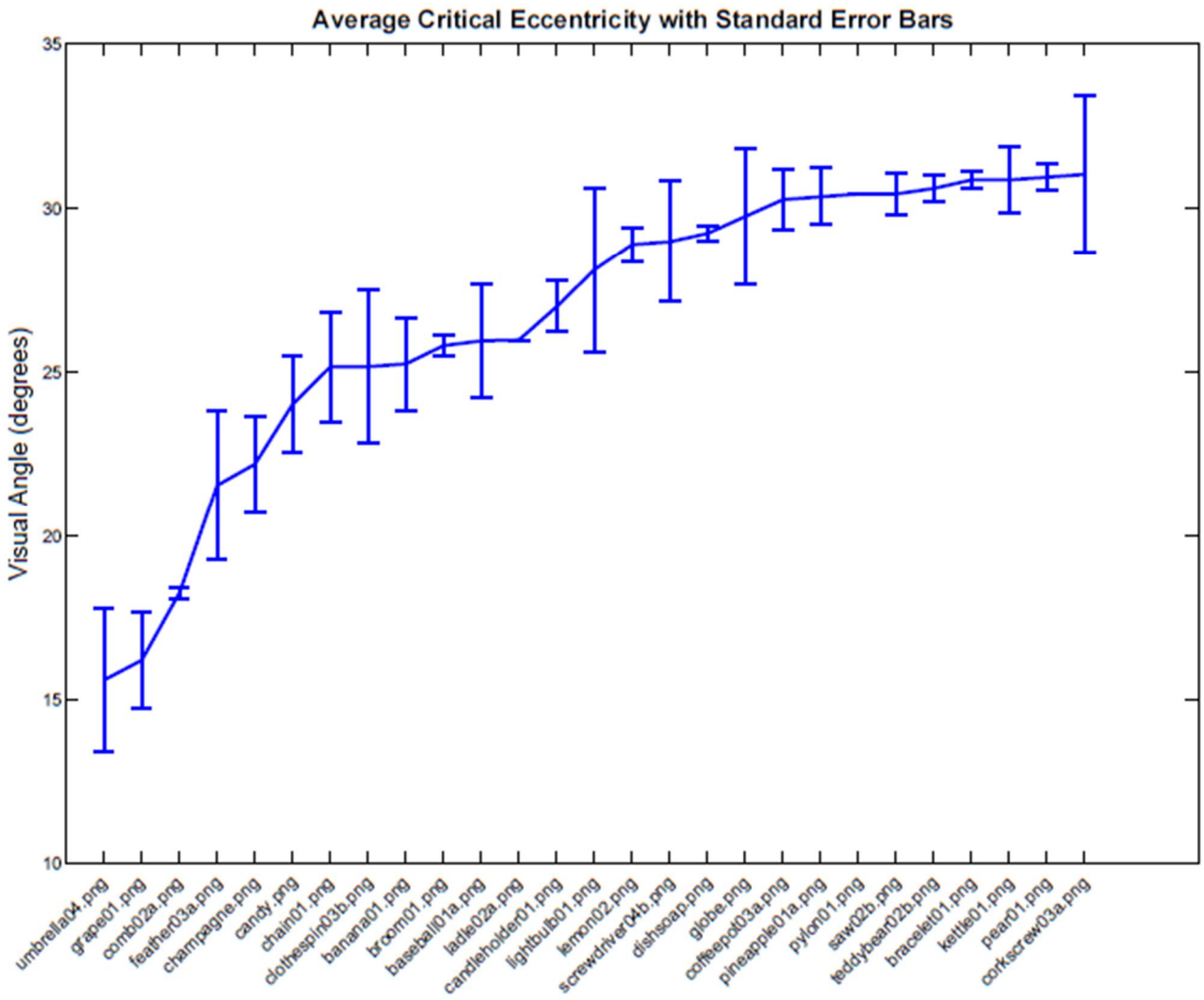

Figure 1. Mean visual angle at which objects were correctly identified across participants, averaged across both visual fields. Objects are ordered from lowest critical eccentricity (closest to fixation) to highest (farthest in the peripheral field). Error bars represent standard error across all subjects.

Figure 2. Pictograph of object stimuli recognized across the range of eccentricity from fixation, binned according to their corresponding CE in px. Averages are based on recognition in the left visual field. Note: images are displayed in color for ease of illustration; experimental stimuli always appeared in grayscale.

Similar to our preliminary behavioral study, stimuli were accurately identified across a consistent and continuous range of eccentricities, ranging from 15° (321 px) from fixation to 31.02° (650 px) when averaged across both visual fields (Figs. 1 & 2). Standard error amongst these locations ranged from 0° to 1.43° (52 px), with an average of 0.67° (25 px; Fig. 1).

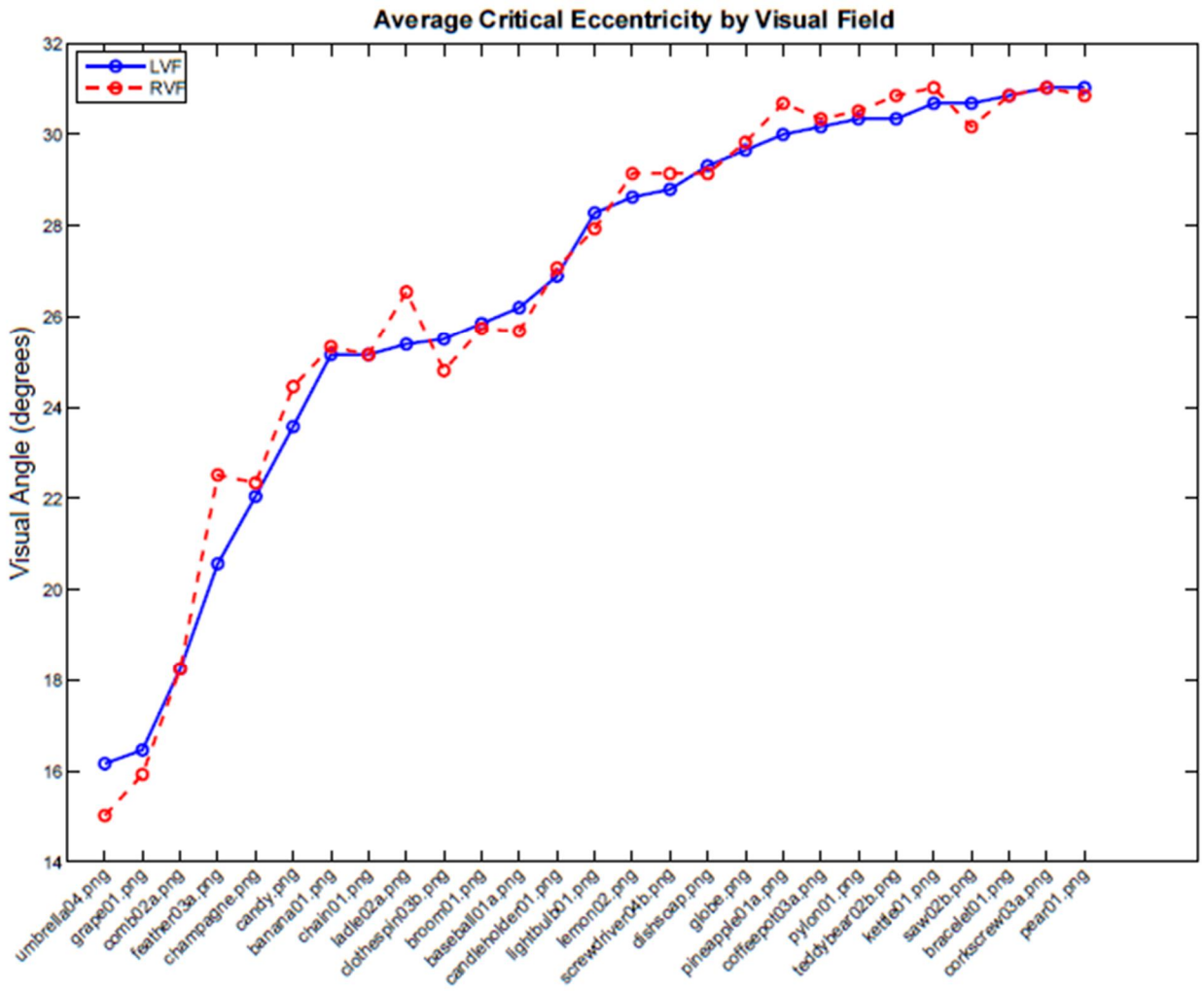

Figure 3. Average critical eccentricities for left (solid blue) and right (dashed red) visual fields. Objects are again arranged in order of increasing critical eccentricity.

Figure 3 shows the difference in average critical eccentricity of objects presented to the left or right visual field. Absolute values of differences ranged from 0° to 1.95° (41.25 px), with a mean of -0.12° (-2.68 px) and a standard deviation of 0.36° (13.07 px). Based on the similarity between CE in both visual fields, subsequent analyses average CE over both visual fields or include information from only the left visual field.

A multiple linear regression investigated the effect of BOSS normative ratings on critical eccentricities averaged across both visual fields for each object. The regression revealed that, of the variables of interest, only familiarity ratings were significantly correlated with average critical eccentricity at the Ŭ= .05 significance level [B = -116.161, $t(43)$ = -2.909, p = 0.0057]. However, this main effect was greatly attenuated when interactions between visual hemifield and

every other variable were added to the model [B = -117.182, $t(34)$ = -1.848, p = 0.0734], and was no longer significant at Ŭ= .05. There were no significant interactions between visual hemifield and BOSS dataset variables (see Appendix F). A comprehensive summary of the original regression results, without interactions, can be found in Table 1.

Table 1

Relation between Normative Ratings and Average Critical Eccentricity

Variable	*B*	*SE B*	*t* value	*p* value
Name agreement	-93.573	68.946	-1.357	0.1818
Category agreement	72.766	70.587	1.031	0.3084
Familiarity	-116.161	39.937	-2.909	0.0057 **
Visual complexity	-4.714	33.544	-0.141	0.8889
Object agreement	64.540	26.539	2.432	0.0193 *
Viewpoint agreement	35.304	27.222	1.297	0.20159
No mental image	2222.643	1163.065	1.911	0.0627 °
Manipulability	-19.577	17.991	-1.088	0.2826
Living/Non-living	-3.150	42.669	-0.074	0.9415
Visual hemifield	2.685	19.755	0.136	0.8925

Notes: R^2 = 0.5404, Adjusted R^2 = 0.4336

Signif. codes: ó**ôp < 0.01, ó*ôp < 0.05, ó°ôp only slightly greater than .05

Table 1. Multiple regression of normative ratings included in the BOSS dataset on average critical eccentricity.

Neuroimaging Data

The main neuroimaging analysis consisted of a group analysis using random effects to identify between-subjects relationships between critical eccentricity and activation in cortical visual processing regions. This random effects analysis was based on the results of a within-subjects analysis for each participant. Individual analyses consisted of a regression in which voxels related to blood oxygenation level dependent (BOLD) signal were correlated with the average critical eccentricities (collapsed over both visual fields) identified for each subject. First,

indicator variables were assigned to every stimulus image: 1 if the image appeared in the trial in question and 0 otherwise. A general linear model (GLM) analysis performed in Statistical Parametric Mapping (SPM) software then assigned beta weights to every indicator variable. This GLM indicated how much the BOLD response changed when each image appeared. These beta weights were then contrasted based on their corresponding values in the critical eccentricity vector. The critical eccentricity vector consisted of normalized measures of CE for each image. The mean value of the eccentricities was subtracted from each eccentricity and then normalized to have a maximum value of 1 without changing the mean. The contrast vector was determined and its results yielded *t* values for every voxel. Finally, these values were used to identify neural regions that responded with greater activation to stimuli at one end of the CE spectrum and negatively to images at the opposite end.

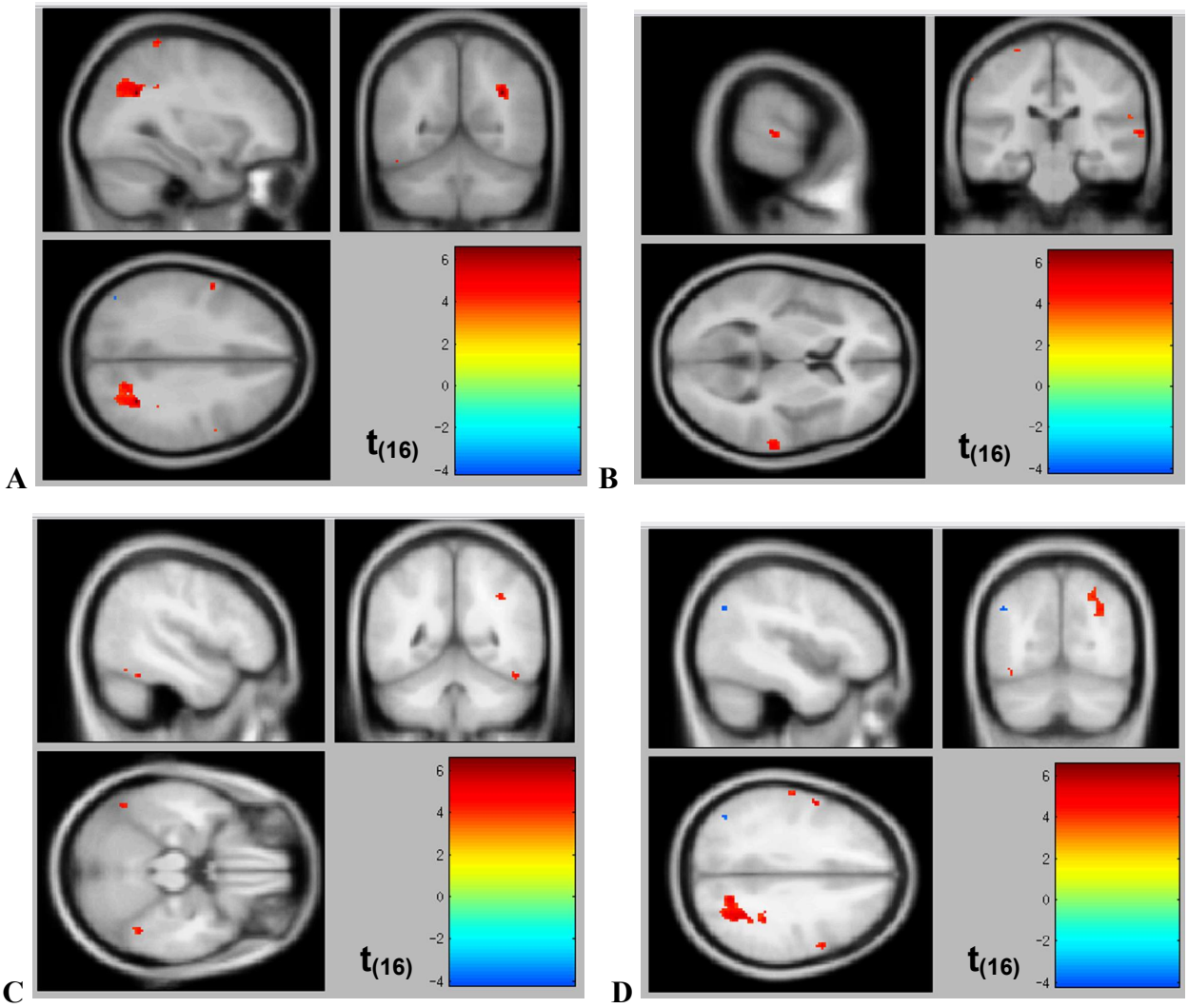

Figure 4. Increased activation to objects with large CEôs (red) in the (A) right parietal lobe, (B) superior temporal gyrus, and (C) bilateral fusiform gyrus. (D) Activation to objects with small CEôs (blue) was found in the left angular gyrus.

The main group contrast revealed four relevant clusters of activation, shown in Figure 4. In response to stimuli with larger CEôs, greater activation was found in the region of the right parietal lobe [Fig. 4.A; peak voxel: x = 32, y = -56, z = 32; total number of voxels = 431; $t(16) = 6.561$, $p < .001$], the right superior temporal gyrus [Fig. 4.B; peak voxel: x = 66, y = -26, z = 6; total number of voxels = 37; $t(16) = 4.7706$, $p < .001$], and bilateral fusiform gyrus [Fig. 4.C; peak voxel: x = 48, y = -50, z = -22; total number of voxels = 13; $t(16) = 4.1643$, $p < .001$]. In contrast, the left angular gyrus [Fig. 4.D; peak voxel: x = -44, y = -70, z = 36; total number of voxels = 13; $t(16) = -3.9686$, $p < .001$] showed greater activation in response to objects with

smaller CEôs. Neuroimaging results are also provided in Table 2 for ease of reference. Complete SPM reports for both positive and negative contrasts are provided in Appendices G and H.

Table 2.

Peak Voxels ($p_{uncorrected} < .001$) for Whole-Brain Holistic vs Configural Contrast

Brain Region	X	Y	Z	*t*	Cluster
Right parietal lobe	32	-56	32	6.651	431
Right superior temporal gyrus	66	-26	6	4.7706	37
Bilateral fusiform gyrus	48	±50	-22	4.1643	13
Left angular gyrus	-44	-70	36	-3.9686	13

Table 2. Peak voxels of activation for whole-brain contrast.

Discussion

This study investigated the mechanisms behind object recognition through a combination of behavioral and neurological methodologies and visual processing theory. Behaviorally, it is believed that the extent of visual crowding is indicative of the number of discrete parts as interpreted by the visual system (Martelli, Majaj, & Pelli, 2005; Pelli & Tillman, 2008). Furthermore, it is likely that such distinctions would also be reflected in brain activity, as previous literature has identified specific regions related to either whole object perception (Kubilius, Wagemans, & Beeck, 2011; Lerner, Hendler, Ben-Bashat, Harel, & Malach, 2001) or individual items or features (Xu & Chun, 2007). In addition, hemispheric lateralization of the perception of parts and wholes has been reported by several studies (Delis, Robertson, & Efron, 1986; Robertson, Lamb, & Knight, 1988) and may play a role in further distinguishing the cerebral processes employed when recognizing objects with varying amounts of discrete visual features. The current study drew upon these premises in an attempt to identify and explain differences in recognition based on the natural part-whole structure of real-world objects.

Behavioral Data

Of the normative ratings regressed against CE values, only familiarity was statistically significant at a 95% confidence level [B = -116.161, $t(43)$ = -2.909, p = 0.0057]. The direction of the relation indicates that, as familiarity ratings increased, CE decreased. Previous literature suggests a connection between expertise and holistic perception ï the more experience an observer has with a given stimulus, the more likely they are to perceive it as global whole

(Richler, Wong, & Gauthier, 2011; Wong et al., 2012). This would lead us to predict that more familiar objects are easier to perceive at large eccentricity from fixation because they are being recognized holistically. However, the data indicate the opposite relation. This may be related to the manner in which the data were analyzed. A recent study of visual crowding and perceptual holism indicated that objects with particularly small CEôs may not be accurately captured by a consistent, monotonic relationship between parts-based and holistic processing (Roldan & Cate, in preparation). This suggests that there may be a minimum eccentricity limit, beyond which our method cannot faithfully index parts-based processing as it relates to holism. Future analyses might address this possibility by examining subsets of the total range of CEôs independently in order to test whether the relationship between CE and holism is nonlinear (see Future Work).

Configural Processing & Hemispheric Lateralization

Although hemispheric bias in part- and whole-based perception has been observed in both behavioral and neuroimaging tasks, empirical findings have been mixed and inconclusive regarding the reliability of its effects; particularly in behavioral studies (Yovel, Yovel, & Levy, 2001). The results of the current study are similarly conflicting. Our behavioral analysis revealed that the effect of visual hemifield on CE was not statistically significant at Ŭ= .05 [B = 2.685, $t(43) = 0.136$, $p = 0.8925$; Table 1]. Therefore, our behavioral results failed to reveal evidence of hemispheric bias in recognition. However, it is important to note that the current study involved no *a priori* prediction regarding which objects may be processed as being more parts-based than others, and the Critical Eccentricity task required focused attention without conflict or divided attention. According to Yovel and colleaguesô previous research, it is unlikely that our design met the proposed criteria for finding robust lateralization biases (Yovel, Yovel, & Levy, 2001). Based on their analysis, if we were interested in finding evidence of hemispheric asymmetry, we might impose attentional conflict by presenting two images simultaneously, one in each hemifield, using stimuli with inherent local or global properties, such as Navon figures (Navon, 1977). These design elements are thought to impose stronger conflict between global and local level processing, and would thereby increase the likelihood of observing robust lateralization effects in perception.

However, neuroimaging results did show at least partial evidence of hemispheric lateralization. The one region of interest (ROI) indicated by our analysis as positively correlated with small-eccentricity objects was located in the left hemisphere; specifically, in the left angular

gyrus (Fig. 4.D). This result aligns with the patterns previously observed by Robertson and others, who have found biases toward local feature perception/detection in the left hemisphere and global bias in the right (Delis, Robertson, & Efron, 1986; Robertson, Lamb, & Knight, 1988). In addition, this finding is similar to those reported by Xu & Chun, who evaluated neural activation when participants viewed perceptually grouped items and found that BOLD response in the inferior IPS decreased when items were grouped (2007). Although the ROIôs in that study were separately tested and identified for each individual subject, an example observer included in the final report shows the inferior IPS located bilaterally in the posterior region of the brain, along z-coordinate 32 (Xu & Chun, 2007, Fig. 3C). Our result, localized to the left angular gyrus [Fig. 4.D; peak voxel: x = -44, y = -70, z = 36; $t(16) = -3.9686$, $p < .001$], although slightly more anterior, falls along a very similar point on the z-axis as that revealed by Xu & Chunôs example observer. Furthermore, our analysis identified this region as an area that exhibited not only increased activation in response to object images with smaller average CEôs, but also decreased activation during trials with large-eccentricity objects. According to visual processing and crowding theory, objects with small CEôs are thought to be perceived configurally, as a collection of discrete features rather than a grouped whole. Based on these results, combined with the evidence for left hemisphere bias in local feature processing, it appears that the left angular gyrus may play a significant role in recognizing objects with more salient part-based structure.

Local Features vs. Configural Structure

When interpreting the evidence for biases toward local feature detection, it is important to consider whether there is a difference between the detection of local features and their global configuration as regarded by the existing literature. Of note is the fact that, in many visual studies aimed toward local vs. global perception, Navon figures (Navon, 1977; Fig. 5) are employed as the primary experimental stimuli. These simple diagrams most often consist of alphabetical characters arranged in such a way as to create a distinct global shape, and thus exhibit an inherent hierarchy of shape level. In the examples below, the local level is represented by a single unit (ôFô in the left image), whereas the global level encompasses the letter created by the combination of multiple units (ôTô in the left image).

Figure 5. Examples of Navon figures. Reproduced from Navon, 1977.

In a Navon figure, the local features are quite clearly recognizable, nameable components: alphabetical characters. However, human object recognition processes do not necessarily operate upon the same principle. Objects, by their very definition, are single, whole exemplars of a nameable unit (e.g., a hammer, kettle, or flower). Although some objects may lend themselves to being further deconstructed into nameable component parts (e.g., handle, spout, or stem), it is not necessarily the case that the visual system relies on such independent, nameable regions in order to facilitate perception. Rather, recognition may be guided by abstract features such as curvature, contrast, texture, or shape occlusion (Biederman, 1987; Logothetis & Sheinberg, 1996). Therefore, it is not entirely appropriate to compare findings related to the recognition of Navon figures to those associated with real-world object recognition. Because of the inherent differences in the structure of objects and Navon figures, such as nameable components and a lack of direct physical connection between components in the latter, it is reasonable to expect that the results of the current study may vary from those described in previous laterality research investigating Navon figure perception.

Holistic Processing

In contrast to the region of the left parietal lobe indicated in the perception of parts-based objects, the right parietal lobe was implicated in the processing of objects with large CEôs [Fig. 4.A; peak voxel: x = 32, y = -56, z = 32; $t(16) = 6.561$, $p < .001$]. This right-hemisphere ROI was located in the IPS, deep within the fundus of the sulcus. It was also closer to the midline of the brain and more anterior and inferior than the left-hemisphere region associated with local-level processing. This cluster in the right posterior parietal lobe responded with increased activation when participants viewed objects that were easily identified at large eccentricity and decreased activation to objects with small CEôs. Again, this result matches those of previous studies that found global level processing biased toward the right hemisphere (Delis, Robertson, & Efron, 1986; Robertson, Lamb, & Knight, 1988). Additionally, this bias further reinforces the principle

behind crowding theory which suggests that objects that are easily recognizable in peripheral vision are processed holistically and do not rely heavily on the detection of multiple discrete visual features (Martelli, Majaj, & Pelli, 2005; Pelli & Tillman, 2008).

In addition, both the right superior temporal gyrus [Fig. 4.B; peak voxel: x = 66, y = -26, z = 6; $t(16) = 4.7706$, $p < .001$] and bilateral fusiform gyrus [Fig. 4.C; peak voxel: x = 48, y = -50, z = -22; total number of voxels = 13; $t(16) = 4.1643$, $p < .001$] demonstrated increased activation when viewing large-eccentricity objects. Previous studies implicate the superior temporal gyrus in auditory functions such as phonetic feature encoding involved in speech processing (Chang et al., 2010; Mesgarani, Cheung, Johnson, & Chang, 2014). It is possible that participants tended to mentally name holistically-perceived objects more often than parts-based ones. However, activation in the superior temporal gyrus corresponds to the reception of speech sounds, and there does not seem to be evidence for the same result to be elicited by silent mental speech alone. The bilateral fusiform gyrus, on the other hand, has commonly been found to be associated with the perception of both face and object stimuli (Kanwisher & Yovel, 2006; McCarthy, Puce, Gore, & Allison, 1997). Although the fusiform gyrus has been shown to exhibit increased activation in response to both objects and face stimuli, one study purports that only a small, specific region in the right lateral fusiform gyrus is associated with face-specific processing (McCarthy, Puce, Gore, & Allison, 1997). More generally, this region is thought to be involved in multisensory integration during object recognition (e.g. haptic, auditory, and visual cues), but areas in the left fusiform gyrus may also be activated during unisensory processing in a single modality alone (Kassuba et al., 2011). Since our stimulus set did not include human faces (only the photograph of a toy bear depicted a conventional face), it is unlikely that this region was acting to facilitate facial processing. Given that the fusiform gyri exhibited increased activation in response to large-eccentricity objects, it is possible that holistically perceived objects tend to have stronger multimodal associations such as naming or manipulablity. However, the results of our regression analysis failed to support this connection because neither name agreement [$B = -93.573$, $t(43) = -1.357$, $p = .1818$] nor manipulability [$B = -19.577$, $t(43) = -1.088$, $p = .2826$] ratings were significantly correlated with CE measures (Table 1).

We hypothesized that 1) the LOC in the ventral occipital-temporal stream would show greater activation during the presentation of objects perceived holistically (i.e., objects with larger CEôs), 2) these holistic objects would elicit a greater amount of general activation in the

anterior regions of the ventral occipital-temporal stream than configural objects, 3) configural objects would correlate with increased parietal lobe activity, particularly in the IPS, and 4) the effect of holistic or configural processing would vary according to hemisphere, with greater activation in the left hemisphere associated with parts-based processing and right hemisphere with global shape processing.

Overall, our hypotheses were partially supported by the data. The presence of bilateral increased activation in the fusiform gyrus, which is considered part of the LOC (Grill-Spector, Kourtzi, & Kanwisher, 2001), in response to large-eccentricity objects supports our initial hypothesis that the LOC would show greater response to objects with larger average CEôs (Hypothesis 1). This result is particularly noteworthy due to its small size and specific localization to the fusiform gyrus. In a popular and influential article, Kanwisher and colleagues proposed that an area of the fusiform gyrus was specialized particularly for face perception, and came to be known as the fusiform face area (FFA; Kanwisher, McDermott, & Chun, 1997). In their initial study, the researchers isolated brain regions that responded with greater activation to faces than objects. Results revealed FFA activation bilaterally in half of 10 right-handed subjects and only in the right hemisphere in the other half. Although the exact location of the FFA varied across subjects, the coordinates of bilateral fusiform gyrus activation identified by the current study are very similar to the FFA coordinates of some of Kanwisherôs participants. Since its inception, the existence and function of the FFA has been the topic of much debate. However, the results of the current study revealed regions of activation overlapping or lateral to the location of the FFA, suggesting that this region is not specific to face perception alone, as increased activation was elicited by images of inanimate, nonhuman objects. Rather, our data supports the contenders of the FFA who argue that the region is responsible for certain categorical processes that apply to both object and face recognition, but which happen to be recruited most heavily during face processing (Ishai, Ungerleider, Martin, Schouten, & Haxby, 1999; Joseph & Gathers, 2002). Indeed, previous studies have also found areas of the fusiform gyrus that respond preferentially to images of objects as opposed to faces (Haxby et al., 2001; Pourtois, Schwartz, Spiridon, Martuzzi, & Vuilleumier, 2009). Haxby and colleaguesôresults showed that, similar to faces, non-face objects ï in their case, chairs ï were capable of activating specific regions in the fusiform gyrus. However, components of the theory behind the FFA serve to reinforce the connection between visual crowding and holistic vs. configural processing. This

is because the prevailing theory regarding face recognition is that faces are processed holistically, as a global whole, rather than by their individual parts (Schiltz & Rossion, 2006; Tanaka & Farah, 1993). If this is the case, and areas of the brain involved in face perception are also recruited by the recognition of objects with large CEôs, it supports our claim that objects less affected by internal feature crowding are represented holistically in the brain. In this way, our study has the potential to serve as a bridge between face-related holism literature and non-face object processing. Whereas previous studies have connected faces to holism/expertise or objects to expertise, the relation of object-processing regions and holism has yet to be fully explored. Our finding regarding object activation in an area of the brain related to holistic processing - the fusiform gyrus - and backed by a behavioral assessment of visual crowding therefore offers an important connection between object perception and holism.

Hypotheses 2 and 3 are also predominantly supported by our findings. Hypothesis 2, predicting that holistic objects would elicit more activation in the anterior ventral occipital-temporal stream than configural objects, is moderately supported by the data. Although it is true that the regions of activation associated with large-eccentricity images were slightly more anterior than the ROI correlated with small-eccentricity stimuli, there are not enough samples of configural ROIôs to confidently support or reject our prediction. Hypothesis 3 is supported insofar as the region activated by configural objects in the left angular gyrus is indeed located in the parietal lobe. However, we did not find significant activation within the IPS, as suggested by Xu & Chun (2007). That being said, it is important to note that the IPS and angular gyrus are physically located adjacent to one another in the brain. Therefore, the discrepancy could be the result of statistical error in identifying the location of the structure, or suggest that regions near the IPS also play a role in configural object recognition.

Finally, Hypothesis 4 regarding hemispheric lateralization, though not supported by behavioral findings, was strongly backed by neuroimaging results. Two ROIôs correlated with large-eccentricity stimuli were located in the right hemisphere, commonly associated with global shape bias (Delis, Robertson, & Efron, 1986; Robertson, Lamb, & Knight, 1988). The third region activated by holistic images appeared bilaterally, in both hemispheres. The single ROI associated with small-eccentricity images was located in the left hemisphere, which is believed to exhibit local level bias in processing. These findings strengthen the claim that holistic and configural processing are lateralized to the right and left cerebral hemispheres. As mentioned

previously, the support provided by our neuroimaging data outweighs the null effect of hemifield on behavioral data, due to our task lacking specific design features thought to facilitate robust behavioral biases (Yovel, Yovel, & Levy, 2001).

Future Work

Further analysis of the current data will aim to create a more complete picture of the interaction between cognitive perceptions and their effects on object recognition processes. Normative ratings from the BOSS dataset will be regressed against brain activation in order to identify any trends between higher-order concepts and neural processing, particularly as they relate to configural or holistic processing areas. In addition, different versions of the fMRI analysis may be performed. The current study utilized a contrast which identified neural regions that responded positively to objects at one end of the CE range and negatively to another. However, it may be helpful to learn which areas were activated positively by either condition, without the added condition of responding negatively to the other. Finally, our behavioral data lead us to believe that the distinction between holistic and configural objects may not exist at the midpoint of the range of CEôs; rather, it is possible that only a small subset of objects at the lowest end of the spectrum may be processed configurally, while all others that fall above that range are collectively perceived holistically. This could explain why there is a sudden increase near the low end of the distribution of behavioral CEôs and fewer ROIôs related to configural processing identified by our neuroimaging analysis. It is our hope that such future analyses will help us better understand parts-based object recognition and its relation to configural and holistic cortical processing regions.

Conclusion

The study of human object recognition is an important endeavor from both an intellectual standpoint and a practical perspective. Like many animals, humans rely on sight in order to interact with their environment on a daily basis. By advancing our understanding of how humans accomplish such automatic tasks as recognizing an object, we not only unlock clues to general and specific processing areas within the brain, but also open the doors to better diagnose and treat disorders in the perception of complex shapes. Our study contributes to the ongoing effort to explain the neural mechanisms that facilitate object recognition as represented by the

perception of distinct parts and global wholes, and its results may serve to enhance our understanding of parts-based and holistic processing in complex shape perception.

References

Aguirre, G. K. (2007). Continuous carry-over designs for fMRI. *NeuroImage*, *35*(4), 1480ï 1494. doi:10.1016/j.neuroimage.2007.02.005

Aguirre, G. (2009, Sept 6). *Pre-made sequences for some stimulus spaces*. Retrieved from https://cfn.upenn.edu/aguirre/wiki/public:premade_sequences

Aguirre, G. (2012, Aug 28). *Sequence generator for Type 1, Index 1 sequences in fMRI.* Retrieved from

Becker, W., & Fuchs, A. F. (1969). Further properties of the human saccadic system: Eye movements and correction saccades with and without visual fixation points. *Vision Research*, *9*(10), 1247ï 1258. doi:10.1016/0042-6989(69)90112-6

Biederman, I. (1987). Recognition-by-components: A theory of human image understanding. *Psychological Review*, *94*(2), 115.

Bouma, H. (1970). Interaction effects in parafoveal letter recognition. *Nature, 226*(5241), 177ï 178. doi:10.1038/226177a0

Brainard, D. H. (1997). The Psychophysics Toolbox. *Spatial vision*, *10*(4), 433ï 436.

Brodeur, M. B., Dionne-Dostie, E., Montreuil, T., & Lepage, M. (2010). The Bank of Standardized Stimuli (BOSS), a new set of 480 normative photos of objects to be used as visual stimuli in cognitive research. *PLoS ONE*, *5*(5). doi:10.1371/journal.pone.0010773

Chang, E. F., Rieger, J. W., Johnson, K., Berger, M. S., Barbaro, N. M., & Knight, R. T. (2010). Categorical speech representation in human superior temporal gyrus. *Nature Neuroscience*, *13*(11), 1428ï 1432. doi:10.1038/nn.2641

Delis, D. C., Robertson, L. C., & Efron, R. (1986). Hemispheric specialization of memory for visual hierarchical stimuli. *Neuropsychologia*, *24*(2), 205ï 214. doi:10.1016/0028-3932(86)90053-9

Dougherty, R. F., Koch, V. M., Brewer, A. A., Fischer, B., Modersitzki, J., & Wandell, B. A. (2003). Visual field representations and locations of visual areas V1/2/3 in human visual cortex. *Journal of Vision*, *3*(10), 1. doi:10.1167/3.10.1

Eger, E., Henson, R. N., Driver, J., & Dolan, R. J. (2007). Mechanisms of top-down facilitation in perception of visual objects studied by fMRI. *Cerebral Cortex*, *17*(9), 2123ï 2133. doi:10.1093/cercor/bhl119

Farah, M. J., Tanaka, J. W., & Drain, H. M. (1995). What causes the face inversion effect? *Journal of Experimental Psychology: Human Perception and Performance*, *21*(3), 628ï 634. doi:10.1037/0096-1523.21.3.628

Grill-Spector, K., Kushnir, T., Hendler, T., Edelman, S., Itzchak, Y., & Malach, R. (1998). A sequence of object-processing stages revealed by fMRI in the human occipital lobe. *Human brain mapping*, *6*(4), 316ï 328.

Grill-Spector, K., & Malach, R. (2004). The human visual cortex. *Annual Review of Neuroscience*, *27*(1), 649ï 677. doi:10.1146/annurev.neuro.27.070203.144220

Haxby, J. V., Gobbini, M. I., Furey, M. L., Ishai, A., Schouten, J. L., & Pietrini, P. (2001). Distributed and Overlapping Representations of Faces and Objects in Ventral Temporal Cortex. *Science*, *293*(5539), 2425ï 2430.

Ishai, A., Ungerleider, L. G., Martin, A., Schouten, J. L., & Haxby, J. V. (1999). Distributed representation of objects in the human ventral visual pathway. *Proceedings of the National Academy of Sciences of the United States of America*, *96*(16), 9379.

Joseph, J. E., & Gathers, A. (2002). Natural and manufactured objects activate the fusiform face area. *Neuroreport May 24, 2002*, *13*(7), 935ï 938.

Kanwisher, N., McDermott, J., & Chun, M. M. (1997). The fusiform face area: A module in human extrastriate cortex specialized for face perception. *The Journal of Neuroscience*, *17*(11), 4302ï 4311.

Kassuba, T., Klinge, C., Hölig, C., Menz, M. M., Ptito, M., Röder, B., & Siebner, H. R. (2011). The left fusiform gyrus hosts trisensory representations of manipulable objects. *NeuroImage*, *56*(3), 1566ï 1577. doi:10.1016/j.neuroimage.2011.02.032

Kourtzi, Z., & Kanwisher, N. (2001). Representation of perceived object shape by the human lateral occipital complex. *Science (New York, N.Y.)*, *293*(5534), 1506ï 1509. doi:10.1126/science.1061133

Kubilius, J., Wagemans, J., & Beeck, H. P. O. de. (2011). Emergence of perceptual gestalts in the human visual cortex: The case of the configural-superiority effect. *Psychological Science*, *22*(10), 1296ï 1303. doi:10.1177/0956797611417000

Lerner, Y., Hendler, T., Ben-Bashat, D., Harel, M., & Malach, R. (2001). A hierarchical axis of object processing stages in the human visual cortex. *Cerebral Cortex*, *11*(4), 287ï 297. doi:10.1093/cercor/11.4.287

Lerner, Y., Hendler, T., & Malach, R. (2002). Object-completion effects in the human lateral occipital complex. *Cerebral Cortex*, *12*(2), 163ï 177. doi:10.1093/cercor/12.2.163

Logothetis, N. K., & Sheinberg, D. L. (1996). Visual Object Recognition. *Annual Review of Neuroscience*, *19*(1), 577ï 621. doi:10.1146/annurev.ne.19.030196.003045

Malach, R., Reppas, J. B., Benson, R. R., Kwong, K. K., Jiang, H., Kennedy, W. A., é Tootell, R. B. (1995). Object-related activity revealed by functional magnetic resonance imaging in human occipital cortex. *Proceedings of the National Academy of Sciences*, *92*(18), 8135ï 8139.

Martelli, M., Majaj, N. J., & Pelli, D. G. (2005). Are faces processed like words? A diagnostic test for recognition by parts. *Journal of Vision*, *5*(1). doi:10.1167/5.1.6

McCarthy, G., Puce, A., Gore, J. C., & Allison, T. (1997). Face-Specific Processing in the Human Fusiform Gyrus. *Journal of Cognitive Neuroscience*, *9*(5), 605ï 610. doi:10.1162/jocn.1997.9.5.605

Mesgarani, N., Cheung, C., Johnson, K., & Chang, E. F. (2014). Phonetic feature encoding in human superior temporal gyrus. *Science*, *343*(6174), 1006ï 1010. doi:10.1126/science.1245994

Mevorach, C., Humphreys, G. W., & Shalev, L. (2005). Attending to local form while ignoring global aspects depends on handedness: Evidence from TMS. *Nature Neuroscience*, *8*(3), 276ï 277. doi:10.1038/nn1400

Navon, D. (1977). Forest before trees: The precedence of global features in visual perception. *Cognitive Psychology*, *9*(3), 353ï 383. doi:10.1016/0010-0285(77)90012-3

Pelli, D. G. (2008). Crowding: A cortical constraint on object recognition. *Current Opinion in Neurobiology*, *18*(4), 445ï 451. doi:10.1016/j.conb.2008.09.008

Pelli, D. G., Farell, B., & Moore, D. C. (2003). The remarkable inefficiency of word recognition. *Nature*, *423*(6941), 752ï 6.

Pelli, D. G., Palomares, M., & Majaj, N. J. (2004). Crowding is unlike ordinary masking: Distinguishing feature integration from detection. *Journal of Vision*, *4*(12), 12. doi:10.1167/4.12.12

Pelli, D. G., & Tillman, K. A. (2007). Parts, wholes, and context in reading: A triple dissociation. *PLoS ONE*, *2*(8), e680. doi:10.1371/journal.pone.0000680

Pelli, D. G., & Tillman, K. A. (2008). The uncrowded window of object recognition. *Nature Neuroscience*, 1129ï 1135. doi:10.1038/nn.2187

Pomerantz, J., & Cragin, A. (2012). Crowding, grouping, and the configural superiority effect. *Journal of Vision*, *12*(9), 1286ï 1286. doi:10.1167/12.9.1286

Pomerantz, J. R., Sager, L. C., & Stoever, R. J. (1977). Perception of wholes and of their component parts: some configural superiority effects. *Journal of experimental psychology. Human perception and performance*, *3*(3), 422ï 435.

Pourtois, G., Schwartz, S., Spiridon, M., Martuzzi, R., & Vuilleumier, P. (2009). Object representations for multiple visual categories overlap in lateral occipital and medial fusiform cortex. *Cerebral Cortex*, *19*(8), 1806ï 1819. doi:10.1093/cercor/bhn210

Reed, C. L., Stone, V. E., Grubb, J. D., & McGoldrick, J. E. (2006). Turning configural processing upside down: Part and whole body postures. *Journal of Experimental Psychology: Human Perception and Performance*, *32*(1), 73ï 87. doi:10.1037/0096-1523.32.1.73

Richler, J. J., Cheung, O. S., & Gauthier, I. (2011). Holistic processing predicts face recognition. *Psychological Science*, *22*(4), 464ï 471. doi:10.1177/0956797611401753

Richler, J. J., Wong, Y. K., & Gauthier, I. (2011). Perceptual expertise as a shift from strategic interference to automatic holistic processing. *Current Directions in Psychological Science*, *20*(2), 129ï 134. doi:10.1177/0963721411402472

Riddoch, M. J., & Humphreys, G. W. (2004). Object identification in simultanagnosia: When wholes are not the sum of their parts. *Cognitive neuropsychology*, *21*(2), 423ï 441. doi:10.1080/02643290342000564

Robertson, L. C., & Lamb, M. R. (1991). Neuropsychological contributions to theories of part/whole organization. *Cognitive Psychology*, *23*(2), 299ï 330. doi:10.1016/0010-0285(91)90012-D

Robertson, L. C., Lamb, M. R., & Knight, R. T. (1988). Effects of lesions of temporal-parietal junction on perceptual and attentional processing in humans. *The Journal of Neuroscience*, *8*(10), 3757ï 3769.

Roldan, S. M., & Cate, A. D. (2014). *Reliability of subjective diagnostic features in real-world objects: A reaction time study*. Manuscript in preparation.

Schiltz, C., & Rossion, B. (2006). Faces are represented holistically in the human occipito-temporal cortex. *NeuroImage*, *32*(3), 1385ï 1394. doi:10.1016/j.neuroimage.2006.05.037

Song, S., Levi, D. M., & Pelli, D. G. (2014). A double dissociation of the acuity and crowding limits to letter identification, and the promise of improved visual screening. *Journal of Vision*, *14*(5), 3. doi:10.1167/14.5.3

Sperry, R. W. (1968). Hemisphere deconnection and unity in conscious awareness. *American Psychologist*, *23*(10), 723ï 733. doi:10.1037/h0026839

Suchow, J. W., & Pelli, D. G. (2013). Learning to detect and combine the features of an object. *Proceedings of the National Academy of Sciences*, *110*(2), 785ï 790. doi:10.1073/pnas.1218438110

Tanaka, J. W., & Farah, M. J. (1993). Parts and wholes in face recognition. *The Quarterly journal of experimental psychology. A, Human experimental psychology*, *46*(2), 225ï 245.

Tootell, R. B., Silverman, M. S., Switkes, E., & Valois, R. D. (1982). Deoxyglucose analysis of retinotopic organization in primate striate cortex. *Science, 218*(4575), 902ï 904. doi:10.1126/science.7134981

Van Essen, D. C., Newsome, W. T., & Maunsell, J. H. R. (1984). The visual field representation in striate cortex of the macaque monkey: Asymmetries, anisotropies, and individual variability. *Vision Research*, *24*(5), 429ï 448. doi:10.1016/0042-6989(84)90041-5

Vuilleumier, P. (2002). Facial expression and selective attention. *Current Opinion in Psychiatry*, *15*(3), 291ï 300. doi:10.1097/00001504-200205000-00011

Whitney, D., & Levi, D. M. (2011). Visual crowding: A fundamental limit on conscious perception and object recognition. *Trends in Cognitive Sciences*, *15*(4), 160ï 168. doi:10.1016/j.tics.2011.02.005

Willenbockel, V., Sadr, J., Fiset, D., Horne, G. O., Gosselin, F., & Tanaka, J. W. (2010). Controlling low-level image properties: The SHINE toolbox. *Behavior Research Methods*, *42*(3), 671ï 684. doi:10.3758/BRM.42.3.671

Wong, A. C.-N., Bukach, C. M., Hsiao, J., Greenspon, E., Ahern, E., Duan, Y., & Lui, K. F. H. (2012). Holistic processing as a hallmark of perceptual expertise for nonface categories including Chinese characters. *Journal of Vision*, *12*(13), 7. doi:10.1167/12.13.7

Xu, Y., & Chun, M. M. (2007). Visual grouping in human parietal cortex. *Proceedings of the National Academy of Sciences of the United States of America*, *104*(47), 18766ï 18771. doi:10.1073/pnas.0705618104

Yovel, G., Yovel, I., & Levy, J. (2001). Hemispheric asymmetries for global and local visual perception: Effects of stimulus and task factors. *Journal of Experimental Psychology: Human Perception and Performance*, *27*(6), 1369ï 1385. doi:10.1037/0096-1523.27.6.1369

Appendix A

Normalized data for experimental stimuli as obtained from the BOSS dataset (Brodeur, Dionne-Dostie, Montreuil, & Lepage, 2010). Reproduced with some omissions.

Filename English	Name agreement	Modal category	Category agreement	Familiarity	Visual complexity	Object agreement	Viewpoint agreement	Manipulability	Living/non-living
banana.jpg	100%	Food	79%	4.7	2.0	4.8	3.8	3.4	L
baseball01a.jpg	87%	Sport	90%	3.8	2.4	4.7	4.8	3.5	NL
bracelet01.jpg	62%	Jewel	53%	3.4	2.2	2.8	3.5	2.9	NL
broom.jpg	94%	Household article	72%	4.3	2.3	4.5	3.0	3.9	NL
candleholder01.jpg	54%	Decoration	71%	3.5	2.5	3.2	3.9	2.0	NL
candy.jpg	95%	Food	87%	4.4	2.1	3.9	3.8	2.3	NL
chain.jpg	95%	Other	44%	3.5	2.2	3.9	3.7	2.2	NL
champagne.jpg	41%	Food	69%	4.3	2.7	4.4	4.5	3.2	NL
clothespin03b.jpg	72%	Household article	57%	4.3	2.3	4.3	3.0	2.6	NL
coffeepot03a.jpg	50%	Kitchen item	87%	4.2	2.3	4.1	4.3	2.2	NL
comb02a.jpg	87%	Bathroom items	90%	4.4	1.9	3.7	2.9	4.1	NL
corkscrew03a.jpg	68%	Kitchen item	90%	3.9	2.4	4.1	4.0	3.3	NL
dishsoap.jpg	42%	Household article	82%	4.4	2.3	4.1	4.2	2.2	NL
feather03a.jpg	100%	Natural	51%	3.9	2.5	4.1	3.7	2.2	NL
globe.jpg	89%	School supply	61%	4.1	3.3	4.6	4.2	2.2	NL
grapes01.jpg	92%	Food	76%	4.6	2.4	3.8	3.9	2.2	L
kettle01.jpg	68%	Kitchen item	82%	4.2	2.2	3.6	4.5	3.1	NL
ladle02a.jpg	57%	Kitchen item	97%	4.2	1.9	4.1	3.5	2.9	NL
lemon02.jpg	100%	Food	82%	4.6	2.2	4.9	4.5	2.1	L
lightbulb01.jpg	83%	Household article	41%	4.5	3.0	4.8	3.9	3.2	NL
pear01.jpg	100%	Food	79%	4.5	2.1	4.8	4.7	1.5	L
pineapple01a.jpg	100%	Food	85%	4.5	3.1	4.8	3.7	1.7	L
pylon.jpg	45%	Other	45%	3.9	1.8	4.6	4.6	2.1	NL
saw02b.jpg	89%	Tool	89%	3.7	2.2	4.3	3.3	4.0	NL
screwdriver04b.jpg	95%	Tool	92%	4.1	2.3	4.5	4.3	3.5	NL
teddybear02b.jpg	72%	Toy	89%	4.1	3.0	4.0	4.2	2.3	NL
umbrella04.jpg	100%	Other	41%	4.5	2.5	3.3	2.4	4.2	NL

Appendix B

Summary of the results from two preliminary behavioral experiments that used crowding techniques to identify critical eccentricities for images from the BOSS database. This report was submitted to the 2013 annual meeting on Object Perception, Attention, and Memory and accepted for presentation as a research poster.

Title: Identifying parts and wholes in real-world objects: an application of critical spacing

Abstract

This study assessed the relative importance of diagnostic parts and holistic shape features in object recognition. Drawing on studies of crowding and isolation fields (Martelli et al., 2005), the critical eccentricity for recognizing normalized photographs of common objects was measured. Objects showed a continuous range of critical eccentricities that were not correlated with higher-order properties such as familiarity or visual complexity, suggesting a holistic/configural continuum. A second experiment asked participants to identify the objectsô most diagnostic regions as well. Results revealed that items with single diagnostic parts were identified among both holistic and parts-based objects.

Summary

A long-standing debate exists among visual neuroscientists regarding the features most useful in object perception. While some advocate holistic processing based on global shapes and configurations amongst features (Tanaka & Farah, 1993), others argue that individual details contain the most important information (Pomerantz, Sager, & Stoever, 1977). These viewpoints, though diametric, are not mutually exclusive, and it is indeed possible that both processing techniques may be involved depending on the stimulus under observation (Martelli, Majaj, & Pelli, 2005).

An informative method for investigating the relative importance of parts and wholes in object recognition recruits crowding as a means to infer the amount of individual parts an image may contain. According to crowding theory, if an object has many parts, these parts will crowd each other at high eccentricities in peripheral vision, thus preventing recognition (Pelli, 2008). Conversely, images processed as one or few parts do not experience crowding and are therefore capable of being recognized at higher eccentricities from fixation. Based on this framework, a group of researchers calculated the minimum critical spacing necessary for an object to be

recognized when flanked by distractors. This distance, termed the isolation field, was found to be roughly half the eccentricity from fixation (Bouma, 1970; Pelli, 2008).

The current study applied the isolation field method to a well-documented database of real-world images. Not only did this allow us to validate the technique using a large and varied set of stimuli, but the quality of the database allowed us to test hypotheses related to 1) the norms recorded for the database objects, which include ratings of high-level semantic properties, and 2) the broad range of local visual features captured by the diverse and well-processed photographs. In line with previous studies, we hypothesized that images perceived as containing multiple parts would require closer proximity to fixation to be correctly identified, whereas objects with fewer parts would be recognized at higher eccentricities. Second, we predicted that these variations in eccentricity at recognition are mediated by visual structure of image features rather than higher-level properties. Finally, we hypothesized that participants would identify diagnostic parts reliably only in objects that were recognized near fixation and less reliably in holistically-perceived objects.

Experiment 1

After providing informed consent, 28 participants named 50 common household objects selected from the BOSS image database (Brodeur, Dionne-Dostie, Montreuil, & Lepage, 2010). After naming each object, participants used a chinrest and fixated a 24ò LCD monitor. To prevent saccades, object images appeared for 150 ms on the left or right side of the screen in a pseudo-random order that prevented stimuli from appearing more than 3 times sequentially on the same side. The experimenter coded participantsô verbal responses as correct/incorrect. Following an incorrect response, an image would appear 75 px (2.8°) closer to fixation on that side of the screen when it next appeared. After a correct response, an imageôs screen position was recorded as the critical eccentricity. Images remained in the cycle and moved closer to fixation until they were correctly identified on both sides of the screen.

Experiment 2

Methods from Experiment 1 were repeated with 23 new participants and a smaller subset of 23 images. After correctly identifying all of the images when presented at eccentricity, participants were required to click on an area of the object that they thought was most recognizable or identifiable for that particular image. Stimuli were presented at fixation briefly (800 ms), followed by a mask overlay that allowed a Gaussian circular window to reveal finite

regions of the image as the subject moved the mouse around the screen. Each object appeared three times in random order. Coordinates of the participant's mouse click were recorded.

Stimuli

Images were presented in grayscale and normalized for luminance and contrast using the SHINE toolbox (Willenbockel et al., 2010). Objects in the final phase of Experiment 2 appeared at 300 px square; all others were displayed at 150 px square.

Results

Eccentricity from fixation at the point of recognition in Experiment 1 was recorded and averaged across participants for each object. A linear regression examined possible correlations with the categories measured by Brodeur and colleagues (2010) including name agreement, category agreement, familiarity, visual complexity, object agreement, viewpoint agreement, manipulability, and living/non-living classification, along with subjective assessments of viewpoint and distortion/foreshortening added by the current researchers. A relationship between average critical eccentricity and frontal parallel viewpoint was found to be significant at $\breve{U} = .05$ ($t = 2.745$, $p = 0.00867$). All other variables bore no significant correlation with average critical eccentricity.

Implications

This study is one of the first to systematically examine part and whole differences in a large set of well-documented images of common objects. The measurements available in the BOSS dataset allow for a detailed examination of whether critical spacing is mediated only by visual structure of image properties or higher-level features. Experiment 1 served as a preliminary, straightforward test of the basic hypothesis that there was no relationship between higher order categories and critical eccentricity. Lack of statistically significant correlations among almost all categories suggests that this technique provides a valid measure for determining parts and wholes as mediated by visual structure for use in further studies of ecologically relevant real-world images. In addition, the study revealed a steady range of critical eccentricity distribution which suggests that the isolation field measure is sensitive enough to distinguish among the subtle differences in part/whole structure found across a varied set of real-world objects. This continuous range also implies that the question of holistic vs. componential processing is not a binary issue; it is important to consider that parts may have different spatial scales. Experiment 2 allowed for the investigation of any systematic relationships between

subjective assessments of features critical to recognition and isolation field size. Results of both studies are expressed qualitatively in Figure 1. Data gained from these experiments provide a strong empirical basis for future studies identifying parts and wholes in object recognition.

Works Cited

Bouma, H. (1970). Interaction Effects in Parafoveal Letter Recognition. *Nature, 226*(5241), 177ï 178. doi:10.1038/226177a0

Brodeur, M. B., Dionne-Dostie, E., Montreuil, T., & Lepage, M. (2010). The Bank of Standardized Stimuli (BOSS), a New Set of 480 Normative Photos of Objects to Be Used as Visual Stimuli in Cognitive Research. *PLoS ONE, 5*(5), e10773.

Martelli, M., Majaj, N. J., & Pelli, D. G. (2005). Are faces processed like words? A diagnostic test for recognition by parts. *Journal of Vision, 5*(1). doi:10.1167/5.1.6

Pelli, D. G. (2008). Crowding: a cortical constraint on object recognition. *Current opinion in neurobiology, 18*(4), 445ï 451. doi:10.1016/j.conb.2008.09.008

Pomerantz, J. R., Sager, L. C., & Stoever, R. J. (1977). Perception of wholes and of their component parts: some configural superiority effects. Journal of experimental psychology. *Human perception and performance, 3*(3), 422ï 435.

Tanaka, J. W., & Farah, M. J. (1993). Parts and wholes in face recognition. *The quarterly journal of experimental psychology. A, Human experimental psychology, 46*(2), 225ï 245.

Willenbockel, V., Sadr, J., Fiset, D., Horne, G., Gosselin, F., & Tanaka, J. (2010). The SHINE toolbox for controlling low-level image properties. *Journal of Vision, 10*(7), 653ï 684.

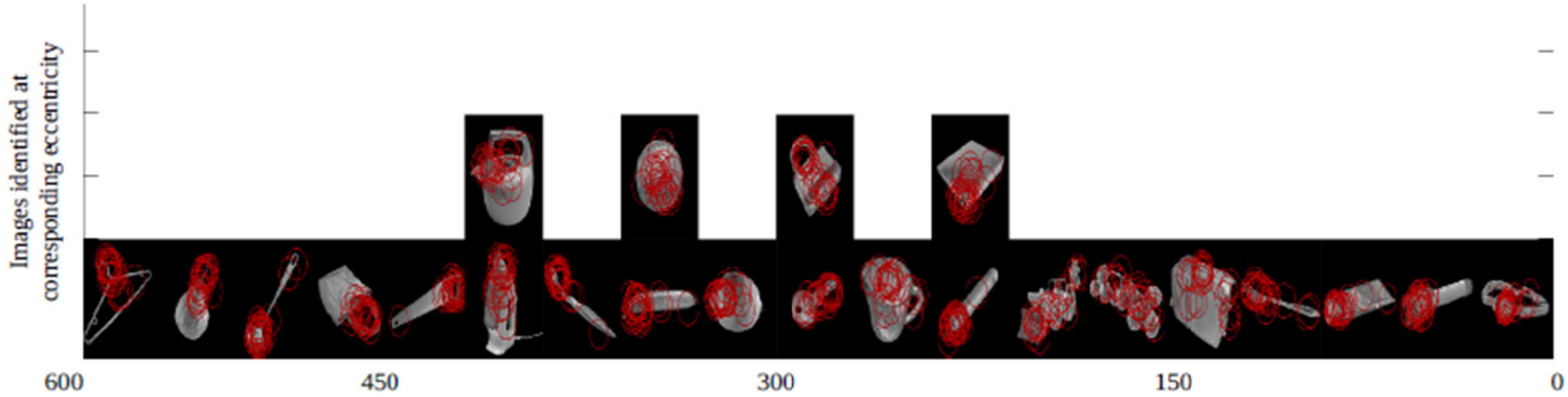

Fig 1. Images are arranged on the x-axis according to their relative critical eccentricities as determined by Experiment 1, with greatest peripheral position on the left. Red circles define the area chosen by subjects as the most identifiable regions of the object as recorded during Experiment 2.

Appendix C

Graph depicting the continuous range of average critical eccentricity values found for images used in Experiment 2 of the preliminary behavioral study (Appendix B).

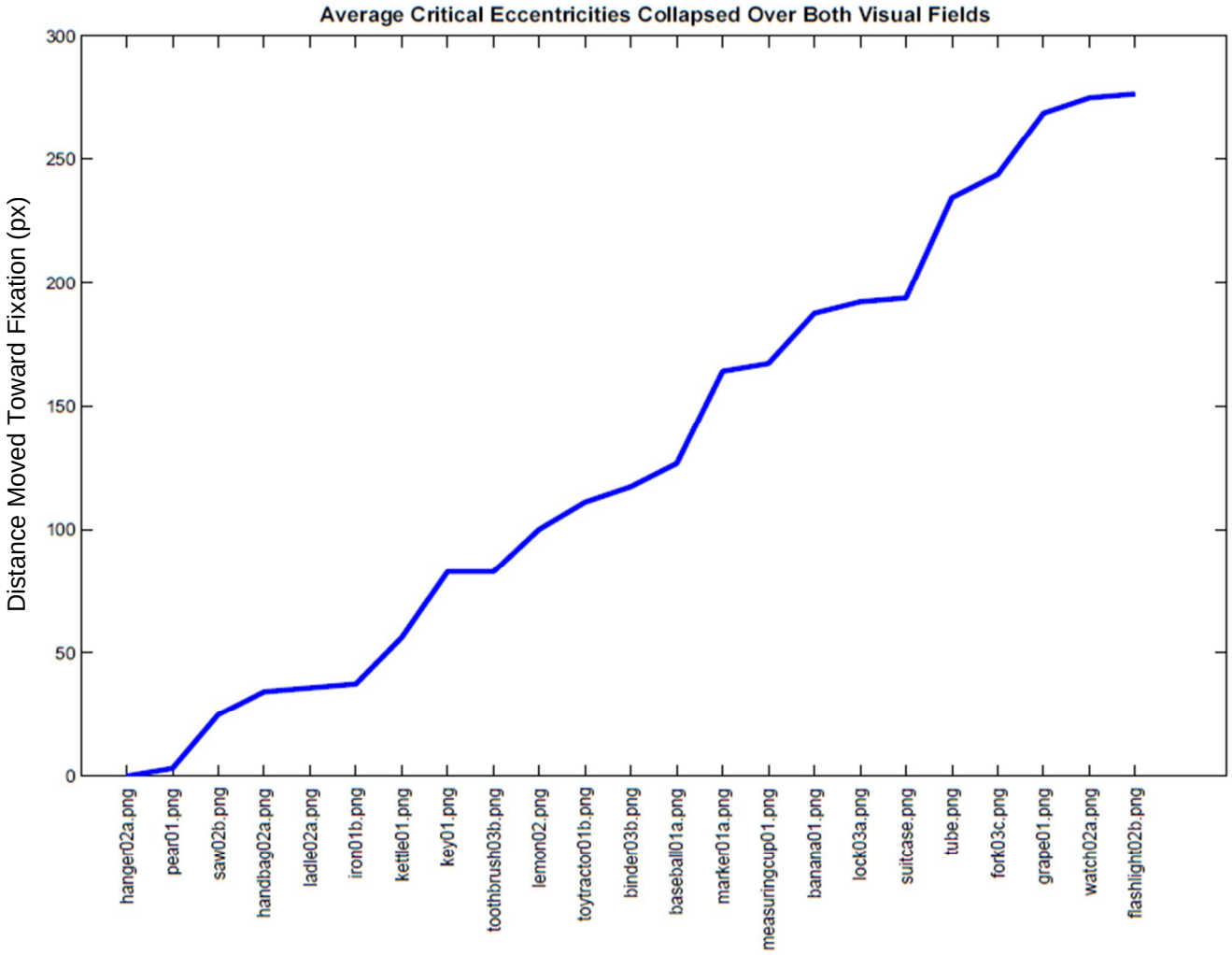

Appendix D

Stimuli as they appeared in the experiment (not to scale).

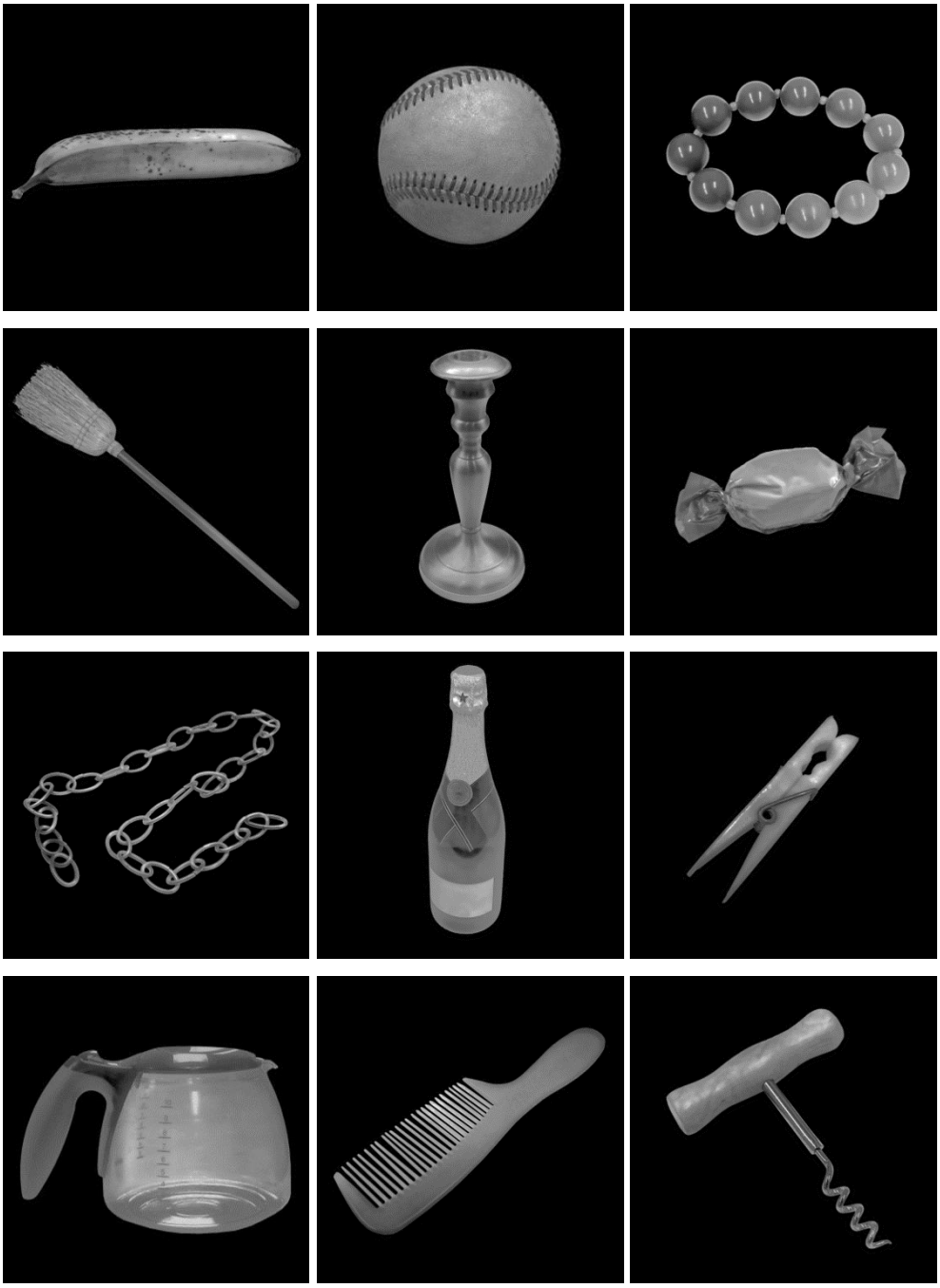

Appendix E

Type 1, Index 1 stimulus sequence used in the neuroimaging phase. Assignment of stimuli to numerical labels is arbitrary; 0 represents null stimuli (black screen with fixation cross visible).

14, 14, 1, 6, 10, 3, 5, 13, 9, 16, 23, 17, 26, 25, 21, 20, 7, 2, 11, 8, 12, 15, 0, 24, 4, 22, 18, 19, 27, 27, 25, 9, 20, 0, 14, 16, 7, 24, 1, 23, 2, 4, 6, 17, 11, 22, 10, 26, 8, 18, 3, 21, 12, 19, 13, 5, 15, 15, 14, 9, 7, 0, 1, 16, 20, 24, 6, 23, 11, 4, 10, 17, 2, 22, 3, 26, 12, 18, 5, 25, 8, 27, 13, 21, 19, 19, 14, 23, 20, 4, 1, 9, 2, 0, 6, 16, 11, 24, 10, 25, 7, 22, 5, 17, 12, 3, 13, 26, 15, 18, 21, 27, 8, 8, 14, 17, 20, 22, 1, 26, 7, 4, 3, 9, 11, 0, 10, 16, 2, 24, 5, 23, 12, 27, 6, 25, 18, 13, 15, 19, 21, 21, 14, 26, 20, 18, 1, 17, 7, 19, 6, 9, 8, 0, 3, 16, 12, 24, 13, 23, 15, 4, 5, 2, 27, 22, 11, 25, 10, 10, 14, 25, 20, 19, 1, 21, 7, 18, 6, 26, 11, 3, 23, 9, 12, 0, 5, 16, 8, 24, 17, 15, 22, 13, 4, 27, 2, 2, 14, 21, 11, 18, 10, 9, 15, 24, 3, 17, 8, 4, 13, 16, 0, 22, 6, 20, 27, 1, 5, 7, 23, 26, 19, 25, 12, 12, 14, 20, 2, 18, 9, 23, 7, 27, 10, 21, 8, 22, 16, 17, 0, 4, 26, 24, 11, 19, 3, 15, 1, 13, 25, 5, 6, 6, 14, 7, 11, 1, 10, 23, 8, 19, 5, 9, 0, 18, 16, 26, 4, 17, 3, 25, 15, 13, 20, 12, 2, 21, 22, 27, 24, 24, 14, 2, 7, 1, 3, 20, 11, 27, 5, 26, 0, 19, 10, 12, 6, 13, 17, 9, 4, 18, 23, 16, 22, 21, 15, 8, 25, 25, 14, 11, 7, 6, 1, 20, 15, 10, 5, 21, 2, 19, 9, 17, 24, 0, 13, 12, 16, 4, 23, 18, 8, 3, 27, 26, 22, 22, 14, 8, 7, 10, 1, 25, 11, 6, 3, 2, 12, 5, 20, 9, 24, 18, 17, 16, 15, 27, 23, 21, 4, 19, 26, 13, 0, 0, 9, 26, 18, 14, 6, 21, 24, 22, 23, 25, 4, 16, 1, 7, 8, 10, 13, 2, 15, 3, 11, 17, 27, 19, 12, 20, 5, 5, 14, 12, 11, 10, 6, 7, 15, 9, 1, 2, 8, 13, 3, 0, 27, 16, 25, 23, 24, 19, 17, 21, 18, 22, 4, 20, 26, 26, 14, 15, 7, 3, 1, 11, 2, 6, 5, 12, 10, 20, 13, 24, 9, 22, 17, 23, 4, 25, 19, 8, 21, 0, 16, 27, 18, 18, 26, 9, 19, 0, 23, 22, 7, 14, 10, 11, 5, 1, 8, 16, 24, 27, 3, 4, 21, 6, 15, 12, 25, 2, 20, 17, 13, 13, 14, 0, 7, 5, 10, 8, 1, 24, 16, 9, 18, 4, 2, 23, 19, 22, 26, 21, 25, 6, 27, 11, 15, 20, 3, 12, 17, 17, 14, 24, 7, 13, 1, 12, 4, 9, 6, 11, 16, 18, 25, 26, 27, 21, 10, 15, 5, 0, 2, 3, 22, 19, 20, 8, 23, 23, 14, 4, 11, 13, 6, 8, 5, 24, 26, 16, 19, 18, 20, 25, 22, 9, 10, 0, 15, 2, 17, 1, 27, 7, 12, 21, 3, 3, 14, 22, 2, 1, 15, 23, 6, 0, 17, 25, 27, 9, 5, 11, 12, 13, 18, 7, 16, 21, 26, 10, 19, 4, 24, 8, 20, 20, 14, 18, 11, 9, 3, 8, 6, 24, 23, 0, 12, 22, 25, 17, 10, 4, 7, 21, 5, 19, 2, 16, 13, 27, 15, 26, 1, 1, 14, 19, 11, 23, 10, 2, 5, 3, 6, 4, 8, 9, 13, 22, 15, 25, 24, 12, 7, 26, 17, 18, 27, 0, 20, 21, 16, 16, 14, 27, 12, 1, 0, 25, 3, 10, 7, 17, 4, 15, 6, 18, 2, 26, 5, 22, 8, 11, 20, 23, 13, 19, 24, 21, 9, 9, 25, 1, 4, 0, 26, 2, 10, 24, 15, 16, 5, 27, 14, 13, 11, 21, 23, 3, 18, 12, 8, 17, 22, 20, 6, 19, 7, 7, 25, 13, 10, 22, 12, 26, 3, 24, 20, 16, 6, 2, 9, 21, 1, 18, 0, 11, 14, 5, 8, 15, 17, 19, 23, 27, 4, 4, 12, 9, 14, 3, 7, 20, 1, 19, 16, 10, 27, 17, 6, 22, 24, 2, 25, 0, 21, 13, 8, 26, 23, 5, 18, 15, 11, 11, 26, 6, 12, 23, 1, 22, 0, 8, 2, 13, 7, 9, 27, 20, 10, 18, 24, 25, 16, 3, 19, 15, 21, 17, 5, 4, 14

Efficiency: 0.39

Appendix F

Complete results of the multiple linear regression conducted on CE and BOSS dataset variables, including interactions with hemifield.

Call:

```
lm(formula = CE ~ name.agree + cat.agree + fam + complex + obj.agree +
    vwpt.agree + nmi + manip + living + VF + VF:name.agree +
    VF:cat.agree + VF:fam + VF:complex + VF:obj.agree + VF:vwpt.agree +
    VF:nmi + VF:manip + VF:living, data = VFCEData)
```

Residuals:

Min	1Q	Median	3Q	Max
-146.78	-32.32	-0.93	38.73	118.1

Coefficients:

	Estimate	Std. Error	t value	Pr(>|t|)	
(Intercept)	718.0762	341.76	2.101	0.0431	
name.agree	-102.471	109.4878	-0.936	0.3559	
cat.agree	62.8218	112.0943	0.56	0.5789	
fam	-117.182	63.422	-1.848	0.0734	.
complex	-2.1373	53.2685	-0.04	0.9682	
obj.agree	64.1711	42.1441	1.523	0.1371	
vwpt.agree	34.7817	43.23	0.805	0.4267	
nmi	2159.587	1846.983	1.169	0.2504	
manip	-14.3898	28.5709	-0.504	0.6178	
livingNL	-10.735	67.7599	-0.158	0.8751	
VF	-13.4988	483.3216	-0.028	0.9779	
name.agree:VF	17.7958	154.8392	0.115	0.9092	
cat.agree:VF	19.8882	158.5252	0.125	0.9009	
fam:VF	2.0414	89.6922	0.023	0.982	
complex:VF	-5.1532	75.3331	-0.068	0.9459	
obj.agree:VF	0.7369	59.6008	0.012	0.9902	

vwpt.agree:VF	1.0443	61.1365	0.017	0.9865
nmi:VF	126.1125	2612.029	0.048	0.9618
manip:VF	-10.3737	40.4054	-0.257	0.7989
livingNL:VF	15.1701	95.827	0.158	0.8752

Signif. codes: 0 '***' 0.001 '**' 0.01 '*' 0.05 '.' 0.1 ' ' 1

Residual standard error: 81.51 on 34 degrees of freedom

Multiple R-squared: 0.5418, Adjusted R-squared: 0.2858

F-statistic: 2.116 on 19 and 34 DF, p-value: 0.02768

Appendix G

Complete SPM report for positive neuroimaging contrast.

Statistics: p-values adjusted for search volume

Cluster-level				Peak-level					
p(FWE-corr)	p(FDR-corr)	equivk	p(unc)	p(FWE-corr)	p(FDR-corr)	T	equivZ	p(unc)	x,y,z {mm}
0	0	431	0	0.374	0.628	6.56	4.51	0	32 -56 32
				0.897	0.668	5.43	4.03	0	20 -64 38
				0.973	0.668	5.11	3.88	0	32 -64 36
0.582	0.342	50	0.033	0.984	0.668	5.01	3.83	0	-56 2 36
				0.991	0.668	4.93	3.79	0	-56 0 44
0.997	0.453	15	0.216	0.993	0.668	4.88	3.76	0	-50 -62 -20
0.804	0.425	37	0.061	0.997	0.668	4.77	3.71	0	66 -26 6
0.994	0.44	17	0.189	0.997	0.668	4.76	3.7	0	-64 -18 38
0.985	0.44	20	0.156	0.999	0.696	4.68	3.66	0	32 -40 70
0.937	0.44	27	0.103	0.999	0.699	4.62	3.63	0	36 -38 36
0.985	0.44	20	0.156	1	0.867	4.34	3.48	0	56 6 36
0.991	0.44	18	0.177	1	0.867	4.28	3.44	0	58 -28 18
0.994	0.44	17	0.189	1	0.867	4.24	3.42	0	-54 -18 54
				1	0.877	4.05	3.31	0	-60 -22 50
1	0.702	6	0.435	1	0.867	4.17	3.38	0	-26 -24 70
0.999	0.473	13	0.248	1	0.867	4.16	3.38	0	48 -50 -22
1	0.777	1	0.777	1	0.918	3.9	3.22	0.001	-60 -4 40
1	0.741	4	0.53	1	0.918	3.9	3.22	0.001	12 -80 -10
1	0.695	7	0.397	1	0.918	3.88	3.21	0.001	46 -62 -20
1	0.717	5	0.478	1	0.918	3.86	3.2	0.001	- 38 -70 -14
1	0.777	1	0.777	1	0.921	3.84	3.18	0.001	-56 4 -8
1	0.777	1	0.777	1	0.955	3.78	3.15	0.001	24 -68 -8
1	0.777	1	0.777	1	0.955	3.76	3.14	0.001	-40 -38 64
1	0.777	1	0.777	1	0.958	3.74	3.12	0.001	42 - 46 -12
1	0.777	1	0.777	1	0.991	3.69	3.09	0.001	8 -78 0

table shows 3 local maxima more than 8.0mm apart

Height threshold: T = 3.69, p = 0.001 (1.000)

Extent threshold: k = 0 voxels, p = 1.000 (1.000)

Expected voxels per cluster, <k> = 10.493

Expected number of clusters, <c> = 26.80

FWEp: 8.217, FDRp: Inf, FWEc: 431, FDRc: 431

Degrees of freedom = [1.0, 16.0]

FWHM = 10.6 10.5 10.2 mm mm mm; 5.3 5.3 5.1 {voxels}

Volume: 2044384 = 255548 voxels = 1664.2 resels

Voxel size: 2.0 2.0 2.0 mm mm mm; (resel = 143.23 voxels)

Appendix H

Complete SPM report for negative neuroimaging contrast.

Statistics: p-values adjusted for search volume

Cluster-level				Peak-level					
p(FWE-corr)	p(FDR-corr)	equivk	p(unc)	p(FWE-corr)	p(FDR-corr)	T	equivZ	p(unc)	x,y,z {mm}
1	0.336	9	0.336	1	0.913	4.13	3.36	0	-40 18 52
0.999	0.336	13	0.248	1	0.913	3.97	3.26	0.001	-44 -70 36

table shows 3 local maxima more than 8.0mm apart

Height threshold: T = 3.69, p = 0.001 (1.000)

Extent threshold: k = 0 voxels, p = 1.000 (1.000)

Expected voxels per cluster, <k> = 10.493

Expected number of clusters, <c> = 26.80

FWEp: 8.217, FDRp: Inf, FWEc: Inf, FDRc: Inf

Degrees of freedom = [1.0, 16.0]

FWHM = 10.6 10.5 10.2 mm mm mm; 5.3 5.3 5.1 {voxels}

Volume: 2044384 = 255548 voxels = 1664.2 resels

Voxel size: 2.0 2.0 2.0 mm mm mm; (resel = 143.23 voxels)